JGR Solid Earth

RESEARCH ARTICLE
10.1029/2018JB016683

Tectonic, Oceanographic, and Climatic Controls on the Cretaceous-Cenozoic Sedimentary Record of the Australian-Antarctic Basin

I. Sauermilch[1], J. M. Whittaker[1], P. K. Bijl[2], J. M. Totterdell[3], and W. Jokat[4]

[1]Institute for Marine and Antarctic Studies, University of Tasmania, Hobart, Tasmania, Australia, [2]Department of Earth Sciences, Faculty of Geosciences, Utrecht University, Utrecht, The Netherlands, [3]Geoscience Australia, Canberra, Australian Capital Territory, Australia, [4]Alfred Wegener Institute for Polar and Marine Sciences, Bremerhaven, Germany

Abstract Understanding the patterns and characteristics of sedimentary deposits on the conjugate Australian-Antarctic margins is critical to reveal the Cretaceous-Cenozoic tectonic, oceanographic, and climatic conditions in the basin. However, unraveling its evolution has remained difficult due to the different seismic stratigraphic interpretations on each margin and sparse drill sites. Here, for the first time, we collate all available seismic reflection profiles on both margins and use newly available offshore drilling data to develop a consistent seismic stratigraphic framework across the Australian-Antarctic basins. We find sedimentation patterns similar in structure and thickness, prior to the onset of Antarctic glaciation, enabling the basinwide correlation of four major sedimentary units and their depositional history. We interpret that during the warm and humid Late Cretaceous (~83–65 Ma), large onshore river systems on both Australia and Antarctica resulted in deltaic sediment deposition offshore. We interpret that the onset of clockwise bottom currents during the early Paleogene (~58–48 Ma) formed prominent sediment drift deposits along both continental rises. We suggest that these currents strengthened and progressed farther east through the Eocene. Coevally, global cooling (<48 Ma) and progressive aridification led to a large-scale decrease in sediment input from both continents. Two major Eocene hiatuses recovered by the Integrated Ocean Discovery Program site U1356A at the Antarctic continental slope likely formed during this preglacial phase of low sedimentation and strong bottom currents. Our results can be used to constrain future paleo-oceanographic modeling of this region and aid the understanding of the oceanographic changes accompanying the transition from a greenhouse to icehouse world.

Key Points:
- This study presents a consistent seismo-stratigraphic framework across the Australian-Antarctic basins using all seismic and drilling data
- During the late Cretaceous deltaic sediments were deposited along both margins, transported by large onshore river systems
- Strengthening ocean currents cause the formation of Paleocene/Eocene contourite drifts and middle-late Eocene winnowing along both margins

Supporting Information:
- Supporting Information S1

Correspondence to:
I. Sauermilch,
isabel.sauermilch@utas.edu.au

Citation:
Sauermilch, I., Whittaker, J. M., Bijl, P. K., Totterdell, J. M., & Jokat, W. (2019). Tectonic, oceanographic, and climatic controls on the Cretaceous-Cenozoic sedimentary record of the Australian-Antarctic Basin. *Journal of Geophysical Research: Solid Earth*, *124*, 7699–7724. https://doi.org/10.1029/2018JB016683

Received 13 SEP 2018
Accepted 22 MAY 2019
Accepted article online 31 MAY 2019
Published online 29 AUG 2019

1. Introduction

The Australian-Antarctic Basin (Figure 1) has formed since the Jurassic. Although continental rifting was initiated in the Middle-Late Jurassic (Bein & Taylor, 1981; Fraser & Tilbury, 1979; Willcox and Stagg, 1990), slow seafloor spreading likely commenced in the Late Cretaceous (~94/83 Ma in the western/central part; Cande & Mutter, 1982), undergoing a significant change in direction and increase in spreading rate at ~47–45 Ma (Close et al., 2009; Whittaker et al., 2007). Coevally, there were drastic climatic and oceanographic changes. Global climate changed from hot "Greenhouse" conditions in the Late Cretaceous, through warm early Eocene, to cold "Icehouse" conditions starting with the first occurrences of Antarctic ice sheets during the middle-late Eocene (e.g., Carter et al., 2017; Gulick et al., 2017; Scher et al., 2014) and large-scale Antarctic glaciation at the Eocene/Oligocene boundary (e.g., Bohaty et al., 2012; Zachos et al., 1994).

Before 50 Ma, the closed tectonic gateways between Antarctica and other continents—Drake Passage and Tasmanian Gateway—caused a circulation featuring two disconnected clockwise gyres: one in the South Atlantic-Indian Ocean, which penetrated into the Australian-Antarctic Basin forming the Proto-Leeuwin-Current, and one in the Pacific Ocean (Huber et al., 2004; McGowran et al., 1997; Sijp et al., 2014). The opening of the Drake Passage remains controversial, and age estimates range from about 49 Ma (Livermore et al., 2005) to ~17 Ma (Barker, 2001). Although the development of the Tasmanian Gateway is better constrained, uncertainties about its evolving paleodepth remain (e.g., Scher et al., 2015). From 50 Ma onward, the shallowly open Tasmanian Gateway allowed penetration of the westward-flowing Tasman Current into the southern parts of the Australian-Antarctic Basin (Bijl et al., 2013; Sijp et al., 2016), which started to connect both gyres. With the continuous widening and deepening

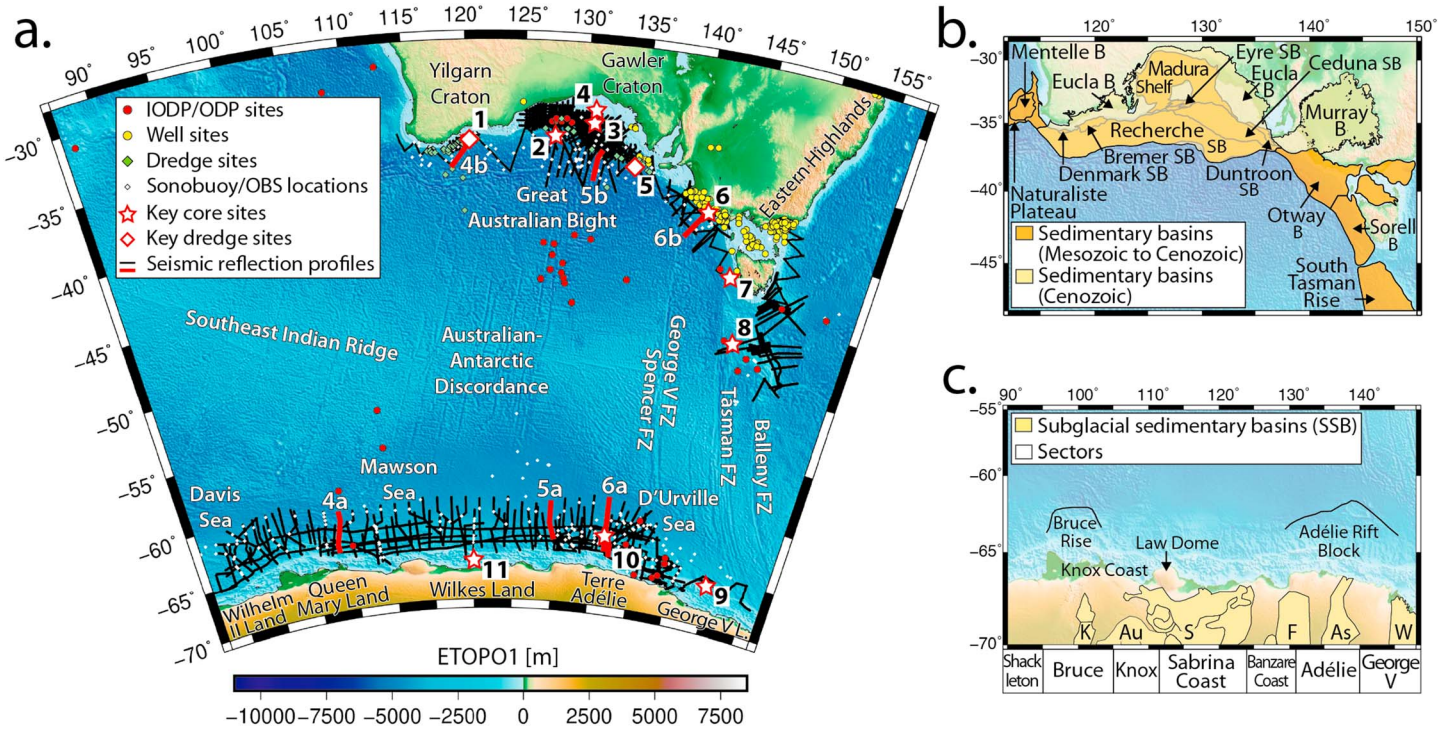

Figure 1. Regional 1-min gravity-derived bathymetric map (ETOPO1; Amante & Eakins, 2009) illustrating the data sets used in this study (a) and main structures (b, c) of the Australian-Antarctic Basin (details, see legends; FZ = fracture zone). Locations of seismic profiles in Figures 4–6 (red lines) and key geological sites: (1) Survey 265, (2) ODP 1128, (3) Jerboa-1, (4) Potoroo-1, (5) Survey 66, (6) Bridgewater Bay-1, (7) ODP 1168, (8) ODP 1170, (9) DF79-38, (10) IODP U1356, (11) Survey NBP14-02 are shown in (a). Sedimentary basins (B = basin, SB = subbasin) after Totterdell and Bradshaw (2004) are shown in (b). Sectors (after Stagg et al., 2004) and subglacial sedimentary basins (SSB; after Aitken et al., 2014): K = Knox SSB, Au = Aurora SSB, S = Sabrina SSB, F = Frost SSB, As = Astrolabe SSB, and W = Wilkes SSB are shown in (c).

of the Tasmanian Gateway, the Proto-Leeuwin Current started to flow into the SW Pacific, leading to the onset of the Antarctic Circumpolar Current (ACC; e.g., Exon et al., 2001). The exact timing of onset and evolving strength of the ACC is still debated. Evidence for rapid deepening of the Tasmanian Gateway around 35.5 Ma suggests the formation of the ACC from ~35 Ma (Bijl, Sluijs, & Brinkhuis, 2013; Sijp et al., 2011; Stickley et al., 2004). However, Scher et al. (2015) propose a tectonic northward shifting of the already deep Tasmanian Gateway into a stronger wind system around 33.5 Ma, triggering the onset of the ACC ~30 Ma. Recent studies suggest that the ACC did not reach its present-day vigor before ~11 Ma (Bijl et al., 2018; Sangiorgi et al., 2018).

The thick sediment succession along the conjugate Australian-Antarctic continental margins is strongly controlled by these tectonic, climatic, and oceanographic processes and so provides a detailed archive for unraveling the evolution of ocean basins and adjacent onshore areas. Most previous workers have investigated the sedimentary architecture on either the Australian or Antarctic margin. Offshore Antarctica, seismic surveys undertaken by different nations have not all been publicly accessible in the past, and so interpretations have been made on separate data collections. Recently, most of these data sets became available through SCAR's Seismic Data Library System (Wardell et al., 2007), enabling a much more integrated seismostratigraphic interpretation work. In addition, new sites were drilled on the East Antarctic margin by the Integrated Ocean Discovery Program (IODP; Leg 318; Escutia et al., 2011; Figure 1a), which for the first time provided key constraints on the age and composition of Eocene and younger sediments (e.g., Bijl et al., 2013, 2018; Tauxe et al., 2012), while new biostratigraphic information helped to refine the interpretation of existing drill cores (ODP sites 269 and 739; Houben et al., 2011, 2013; Passchier et al., 2013). Here we capitalize on the newly available Antarctic seismic and geological information and develop a consistent seismic stratigraphic interpretation for both conjugate Australian-Antarctic margins.

2. Stratigraphic Framework

2.1. Antarctica

Seismic reflection profiles have been collected offshore Wilkes Land since the 1980s. Early stratigraphic interpretations were undertaken based on relatively sparse seismic data mostly in the eastern sectors (Figure 1c) and using constraints from Deep Sea Drilling Project (DSDP) Leg 28 (e.g., Eittreim & Hampton, 1987; Eittreim et al., 1995; Tanahashi et al., 1997; Tsumuraya et al., 1985; Wannesson et al., 1985; Figure 3). These early studies identified a prominent unconformity dividing the sedimentary column into glacial and nonglacial sequences based on characteristic glacial structures, such as channel levees, turbidites, sediment waves, and debris flows (e.g., Donda et al., 2003, 2007; Escutia et al., 2002, 2003). The lowermost unit with strong faulting was interpreted as syn-rift material (Figure 3; Figures 4–6: equal to S1).

In the late 1990s, hundreds of kilometers of multichannel seismic reflection data with deeper signal penetration were collected offshore Wilkes Land (Figure 1a). All marginwide seismic stratigraphic interpretations (Close et al., 2007; Colwell et al., 2006; Leitchenkov et al., 2007; Leitchenkov & Guseva, 2012; Stagg et al., 2005) consistently interpreted a lower prominent reflection as the "breakup" unconformity consistent with initial interpretations (Figure 3; Figures 4–6: equal to U1). Despite a lack of stratigraphic control, most authors consider the timing of the lower unconformity to be Turonian offshore the western and central Wilkes Land, and Maastrichtian offshore Terre Adélie and George V Land (e.g., Close et al., 2007; Leitchenkov et al., 2007; Leitchenkov & Guseva, 2012; Figure 3).

However, significant differences exist regarding the interpretations of a younger prominent unconformity and its formation, which we interpret as two separate unconformities (Figures 3 and 4–6: U2 and U3). This (typically interpreted as) Eocene unconformity features both in marginwide interpretations and also in interpretations focused on younger strata and/or particular sectors of the Antarctic margin (e.g., Brancolini & Harris, 2000; De Santis et al., 2003; Donda et al., 2003; Escutia et al., 1997, 2002).

Eittreim et al. (1995) and Escutia et al. (1997) proposed the onset of widespread continental glaciation, and associated erosion, ~34 Ma as the mechanism driving the formation of this unconformity (Figure 3). Close et al. (2007) described a single unconformity extending along the margin due to a prominent onlapping pattern of the overlying sediment. Based on the presence of a similar unconformity offshore the conjugate Australian margin, they excluded glaciation as a possible formation process. Instead, they argue for a major erosional event at ~45 Ma (Figure 3), caused by the initiation of strong, deep ocean currents enabled by an increasing seafloor spreading rate and synchronous, rapid subsidence of both margins.

Leitchenkov et al. (2007, 2012) extended the interpretation of this unconformity past the Wilkes Land region to almost the entire East Antarctic margin, which excludes a specific tectonic formation process within the Australian-Antarctic sector. They observed a more complex structure of this Eocene formation, interpreting two high-amplitude reflections, which split at a number of locations along the margin. Leitchenkov and Guseva (2012) propose that a drastic global sea level drop of about 70 m caused widescale erosion of the southern Australian and the East Antarctic margins at ~42 Ma (based on Miller et al., 2005), forming the lower horizon. However, for the central and western part of the margin, Leitchenkov et al. (2015) suggest the possibility of nondeposition forming this reflection. The onset of continent-wide glaciation ~34 Ma is proposed as the driver of the second major erosional event (upper horizon; Leitchenkov & Guseva, 2012; Figure 3).

In 2010, IODP Site U1356 (Leg 318, Figures 1a and 6a) was the first geological site offshore East Antarctica to drill through this prominent reflection pattern. This continental rise site (~4,003 mbsl) between the Adélie Rift Block and continental slope, intersected two hiatuses, coinciding with the prominent Eocene unconformity. These hiatuses were constrained to 51.9–51.06 and 47.9–33.6 Ma (Bijl, Bendle, et al., 2013; Escutia et al., 2011; Tauxe et al., 2012). The younger hiatus was interpreted to have formed at ~33.6 Ma via widespread erosion of existing sediments, when the first coastal glaciation led to glaciers grounding on the shelf, erosive downslope bottom currents, and coinciding sea level changes (Escutia et al., 2011; Stocchi et al., 2013). Evidence for abundant reworked Eocene microfossils detected in the lowermost Oligocene sediments at Site U1356 (Bijl, Houben, Bruls, et al., 2018; Houben et al., 2013) and Eocene material in dredge samples offshore the Mertz Glacier (Truswell, 1982) support this interpretation. Escutia et al. (2011) interpreted the

older hiatus (51.9–51.06 Ma) to have formed due to an increased rate of seafloor spreading, as originally proposed by Close et al. (2007).

In summary, all studies propose that massive erosional events formed the younger and/or the older hiatuses by removing 200–600 m of sediment (Close et al., 2007; Eittreim et al., 1995; Escutia et al., 2011; Leitchenkov & Guseva, 2012). The Eocene unconformity is found across wide areas of the East Antarctic (and Australian) margin, which implies that a large amount of eroded sediment would have been redeposited somewhere along the margins. Although the Oligocene sediments at IODP Site U1356 contain reworked Eocene microfossils, the highest abundance is concentrated in the lowermost ~16 m (Houben et al., 2013), which would not be enough to account for ~200–600 m of eroded sediment. To date, no evidence for such large amount of redeposited sediments has been detected in geophysical or geological data.

2.2. Australia

Geologically, the Australian conjugate is much better constrained than the Antarctic margin, by numerous petroleum exploration wells (Figure 1a; Totterdell et al., 2014) and scientific drilling expeditions (DSDP Leg 29: South Tasman Rise and Sorell Basin (Kennett et al., 1974); Ocean Drilling Program (ODP) Leg 182 (Feary et al., 2000); and IODP 369: Great Australian Bight (GAB) [Huber et al., 2018; Leg 189: Tasman Region (Exon et al., 2001)). Early studies based on first well and seismic data led the initial seismostratigraphic interpretations of the Bight and Otway basins in the 1970s (e.g., Boeuf & Doust, 1975; Deighton et al., 1976; Fraser & Tilbury, 1979; Hayes, 1975). Stagg et al. (1990) subdivided the southern Australian margin into major Mesozoic sedimentary basins that formed during the long rift phase (Figure 1b). These basins are largely overlain unconformably by a thin Cenozoic carbonate platform (e.g., Stagg et al., 1990). Comprehensive overviews of each of the basins along the margin, with focus on the shelf and upper slopes, have been undertaken (e.g., Bradshaw, 2005, Bremer Subbasin; Totterdell et al., 2000, GAB; Krassay et al., 2004, Otway Basin; Stacey et al., 2013, Otway and Sorell basins). Although some studies use constraints from neighboring basins, only a few marginwide seismic correlations have been made across all basins. However, helpful syntheses can be found in Blevin and Cathro (2008) and Totterdell et al. (2014).

Although the tectonic evolution of the Bremer, Bight, Otway, and Sorell basins did not occur simultaneously, their overall evolution was similar. Each basin exhibits the transformation from a small, isolated nonmarine, and fluviolacustrine intracratonic rift to a complex marine passive margin system (Figure 2; Blevin & Cathro, 2008). From the Bremer Subbasin in the west to the Sorell Basin in the east, all depocenters contain thick syn-rift nonmarine, fluvio-lacustrine sediment units deposited from about the Middle-Late Jurassic (Bremer Subbasin, central GAB, and western Otway Basin) to Early Cretaceous (Otway and Sorell basins; Bradshaw, 2005; Krassay et al., 2004; Stacey et al., 2013; Totterdell et al., 2000; Totterdell & Bradshaw, 2004). During the Aptian-Albian, increased marine influence is observed in the Bight and Otway basins (based on lithological observations at drill and dredge sites; Figure 2). In most regions, this was followed by the development of thick Late Cretaceous deltaic successions with deposition controlled by both growth faulting and thick-skinned extensional faulting (Robson et al., 2016; Totterdell & Krassay, 2003b). A relatively thin cover (max. ~1,700 m in the Duntroon Subbasin; Totterdell et al., 2000) of Cenozoic marine, dominantly carbonate, sediment is observed (Figure 2).

At the eastern end of the Australian southern margin is the continental South Tasman Rise, which contains small, isolated sedimentary basins (e.g., Hill et al., 2001). This region was partly influenced by different tectonic processes, and therefore, the sediment-stratigraphic evolution shows differences to the rest of the southern Australian margin. However, the same transition from shallow to open marine sedimentation can be observed from the middle-late Eocene (Hill et al., 2001; Figure 2).

Some links between the Australian and Antarctic seismic structures have previously been made (e.g., Ball et al., 2013; Close et al., 2007; Colwell et al., 2006; Espurt et al., 2012; Gillard et al., 2015; Lane et al., 2012). Most of these studies were limited to the central GAB and conjugate Wilkes Land, focusing on the detailed comparison of tectonic structures detected in crustal basement and syn-rift sediments that formed during lithospheric thinning and/or early breakup (Ball et al., 2013; Espurt et al., 2012; Gillard et al., 2015; Lane et al., 2012). Broader comparisons between the overall character of seismic units were made by Close et al., 2007; Colwell et al., 2006; and Leitchenkov et al., 2015.

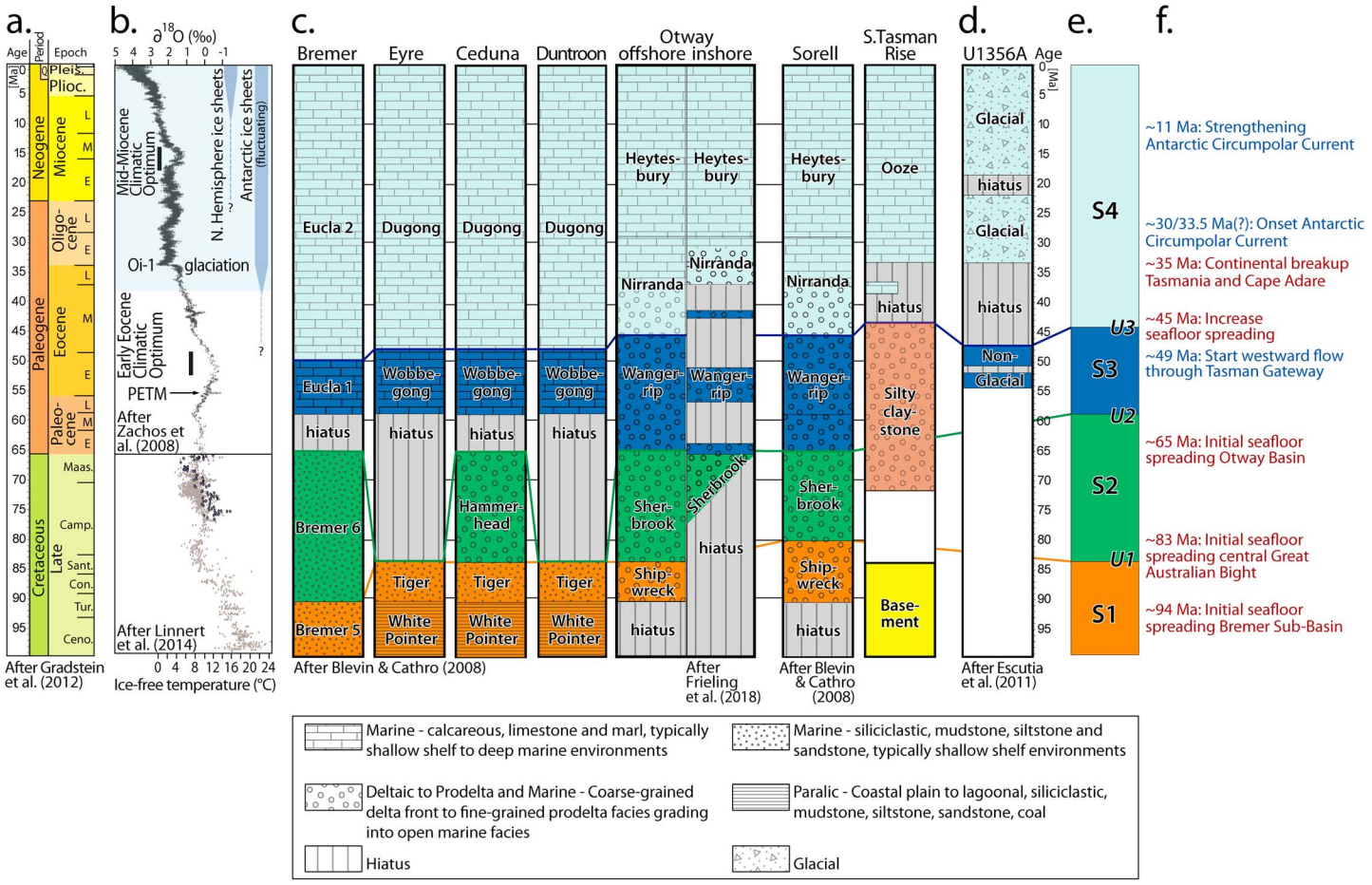

Figure 2. Overview of stratigraphic sequences and depositional environment of the (c) basins along the Australian southern margin (Blevin & Cathro, 2008; Frieling et al., 2018), (d) drill site U1356A, Antarctica (Escutia et al., 2011), and (e) the stratigraphic interpretation (this study). (a) Geological timescale (Gradstein et al., 2012), (b) deep-sea benthic foraminiferal oxygen-isotope curve (Linnert et al., 2014; Zachos et al., 2008), (f) regional tectonic (red), and oceanic (blue) events are shown.

2.3. Uncertainties

Uncertainties in the seismostratigraphic interpretation covering such a large region (this and previous studies) are inevitable in certain areas, due to a lack of geological constraints, decreased resolution of seismic signal in deeper profile sections, different acquisition and processing parameters between seismic surveys, deformation of characteristic older sediment structures due to compaction by thick overlying material, or reflections onlapped or truncated on bathymetric obstacles hampering correlation.

Some areas, particularly along the Antarctic margin, are affected by these factors. As IODP Site U1356 provides the only robust, but stratigraphically limited, geological constraints for preglacial Cenozoic material along this margin, uncertainties increase with distance from this site. The elevated Adélie Rift Block (Figure 6a) causes thinning of sediment units or onlapping of prominent reflections, which leads to some uncertainty. In the George V Sector, submarine volcanoes and seismic profiles with shallow signal penetration cause uncertainties. Farther west along the Antarctic margin, strong structural similarities and margin-parallel tie profiles provide high confidence in the stratigraphic correlation. However, some deeper structures can be strongly compressed by thick overlying material, making the determination of underlying unconformities difficult.

The stratigraphic interpretation offshore southern Australia is better constrained by various geological sites along the shelves, but stratigraphic uncertainty increases basinward where fewer wells have been drilled. In

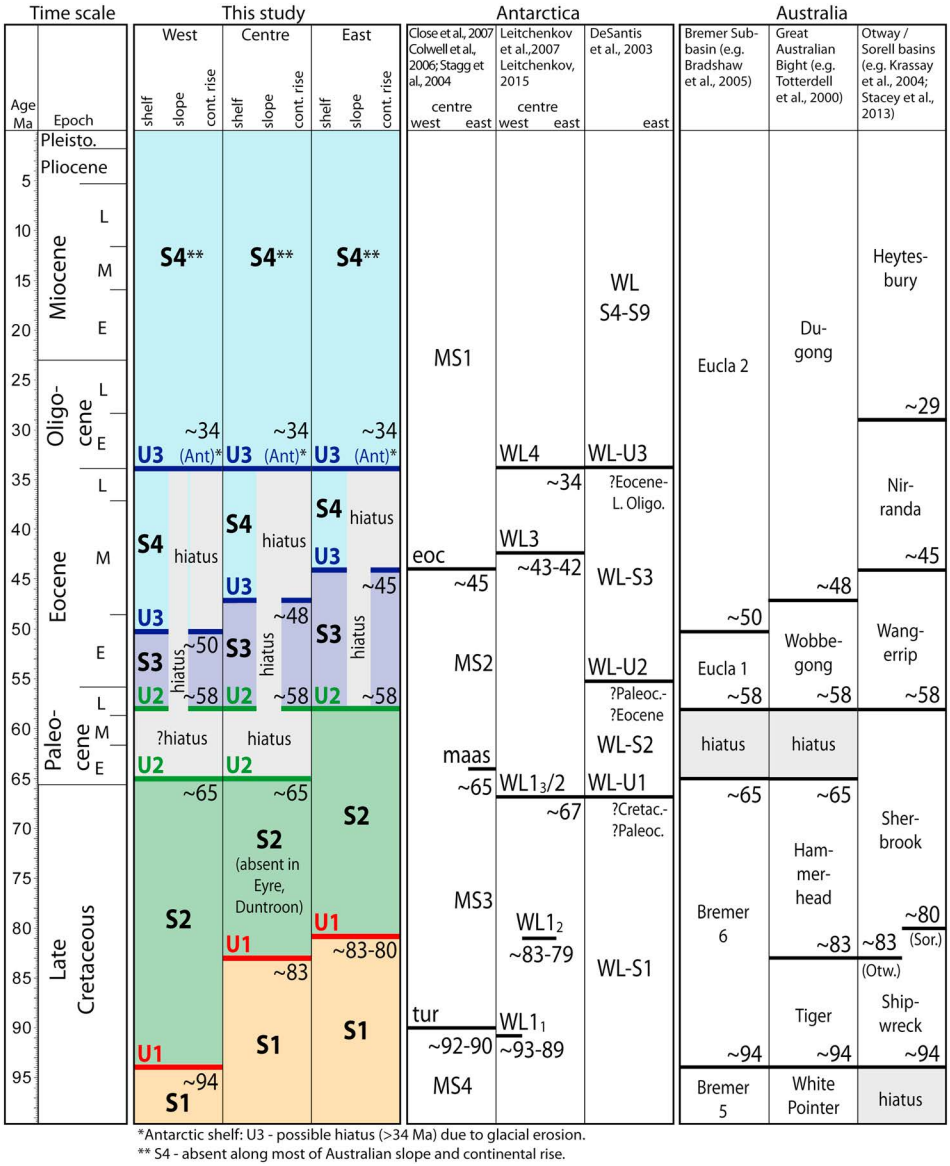

Figure 3. Horizon and sedimentary unit ages interpreted in this study, in comparison with previous key investigations along the Antarctic and Australian margins.

addition, sample coverage decreases toward the continental rise and the lack of margin-parallel seismic profiles causes some uncertainty.

3. Data and Methods

3.1. Multichannel Seismic Reflection Data

Along both Australian and Antarctic margins, about 500 seismic reflection lines (~60,000 km) are analyzed and stratigraphically interpreted in this contribution (Figure 1a). SCAR's Seismic Data Library System (Wardell et al., 2007) provides all existing profiles collected offshore Antarctica from 1980s to 2006. Data sets from seismic surveys acquired offshore Australia are provided by Geoscience Australia (Surveys AGSO 137, 199, 202, 224, S280, 2012 Acreage Release seismic data package) and Spectrum Geo Ltd. (Petrel Roving Survey 1973). The seismic interpretation work was undertaken using IHS Kingdom software (version 2015.0). All seismic profiles are stored and displayed in two-way travel time (s, TWT).

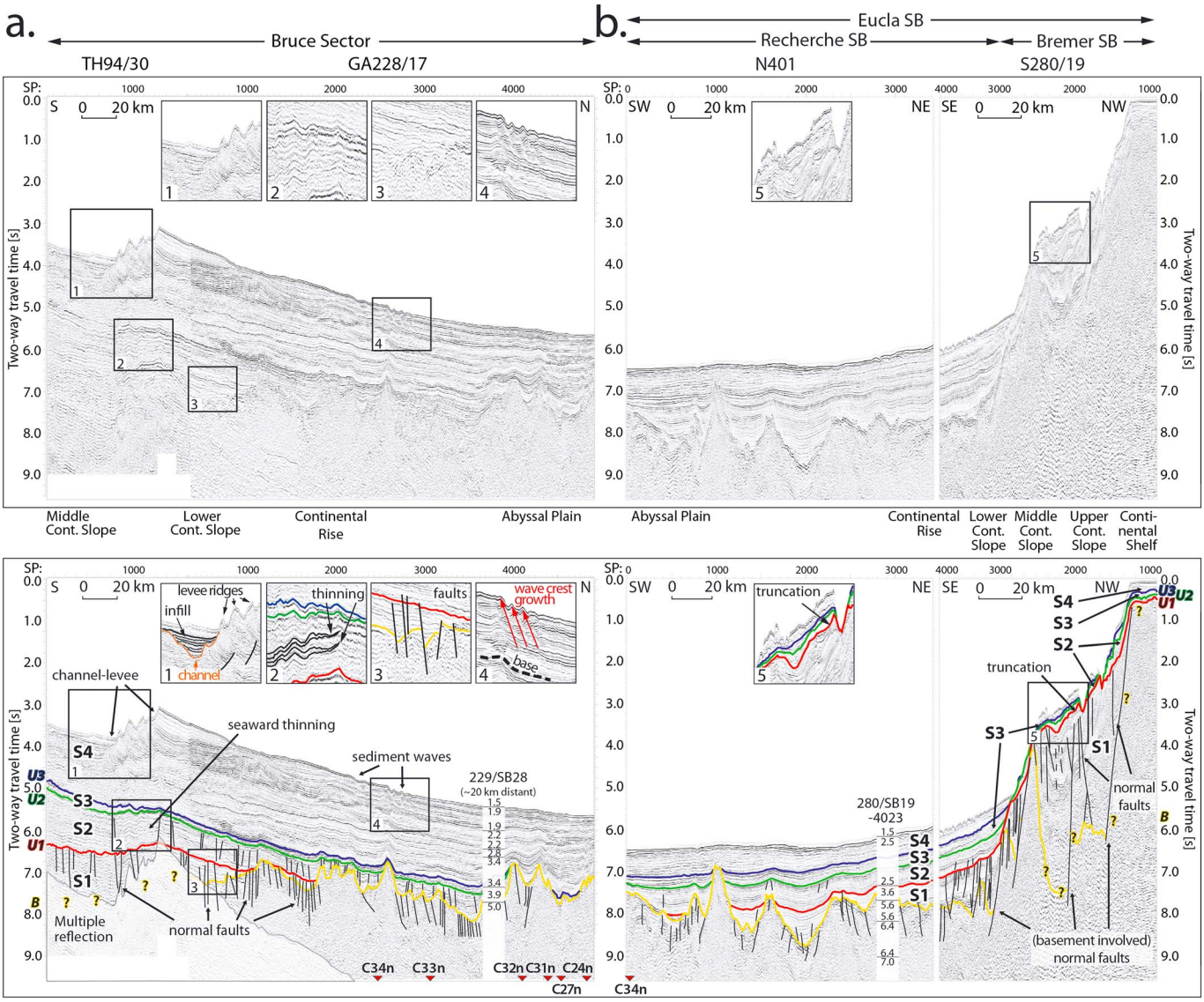

Figure 4. Uninterpreted (top) and interpreted (bottom) conjugate seismic reflection profiles offshore (a) Antarctica and (b) Australia in the western Australian-Antarctic Basin (location, see Figure 1a). Key unconformities: Basement B = yellow, U1 = red, U2 = green, U3 = blue, and sedimentary units S1–S4. Faults = thin black lines. Interval velocity information from sonobuoy locations are shown (in km/s; white box; after Whittaker et al., 2013b). Magnetic anomalies are shown as red triangles (after Whittaker et al., 2007). Characteristic features described in the text are shown in zoom-ins with lower vertical exaggeration (1–5). A high-resolution (1,200 ppi) version of this figure can be found in the supporting information (S1).

On the Antarctic margin, a comprehensive coverage of margin-crossing profiles (distance ranges between ~10 and 150 km; Figure 1a), and in particular, margin-parallel profiles ensures the consistency and accuracy of the stratigraphic interpretation. On the Australian margin, subbasins are not as well linked by seismic profiles, so prominent key reflections and units with strong similar structures and amplitude characteristics are linked together with the aid of geological constraints (Figures 4–6).

3.2. Depth Conversion and Plate Tectonic Reconstruction

The interpreted horizons are exported and used to compute interpolated 0.5° grids in two-way travel time (s). For each key horizon, velocity grids are computed using the interval velocities from in total 1,143 sonobuoy and ocean bottom seismometer stations (after Whittaker, Goncharov, et al., 2013; Figure 1a) as a function of two-way travel time. The interval velocities of the sedimentary units cover the following ranges: (a) S1 from 2.0 to 5.0 km/s, (b) S2 from 2.0 to 4.0 km/s, (c) S3 from 1.6 to 3.5 km/s, and (d) S4 from 1.6 to 2.5 km/s. The

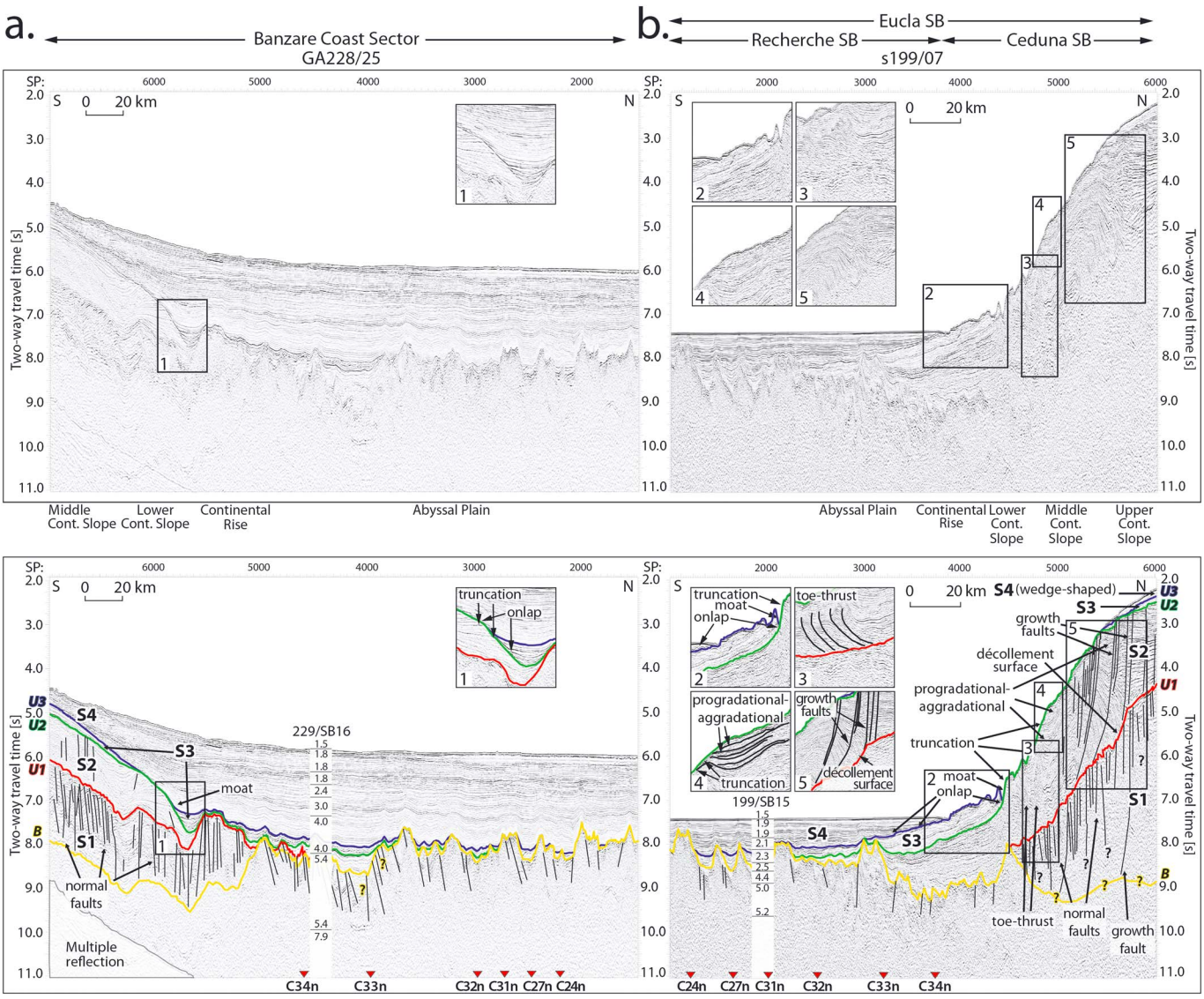

Figure 5. Uninterpreted (top) and interpreted (bottom) conjugate seismic reflection profiles offshore (a) Antarctica and (b) Australia in the central Australian-Antarctic Basin (location, see Figure 1a). Legend as in Figure 4. A high-resolution (1,200 ppi) version of this figure can be found in the supporting information (S2).

velocities depend strongly on the thickness of overlying sediments due to compaction, which causes wide ranges in velocity within each unit (e.g., high S3 velocities [3.5 km/s] offshore parts of Antarctica with thick overlying S4 unit [Figure 10] and lower values [1.6 km/s] for most parts offshore Australia).

Horizon grids in depth (km), sediment thickness ("isopach") grids, and volumes for each unit are calculated and reconstructed back in geological time (Figure 7, 67 Ma; Figure 9, 43.8 Ma) using GPlates 2.0 and the plate model of Whittaker, Williams, et al. (2013).

3.3. Geological Data

For our seismic stratigraphy, geological constraints are taken from various drill, piston core, and dredge sites along both margins (Figure 1a). The correlation between seismostratigraphic interpretation and geological data is crucial to infer ages and depositional environment of the sedimentary units.

Along the Antarctic margin, key constraints are obtained from IODP Leg 318 (Terre Adélie; Escutia et al., 2011), DSDP Leg 28 (Wilkes Land/Terre Adélie; Hayes, 1975), and ODP Leg 183 (Kerguelen Plateau; Coffin et al., 2000). For this study, IODP Site U1356 and U1360 (Leg 318) provide the key constraints on

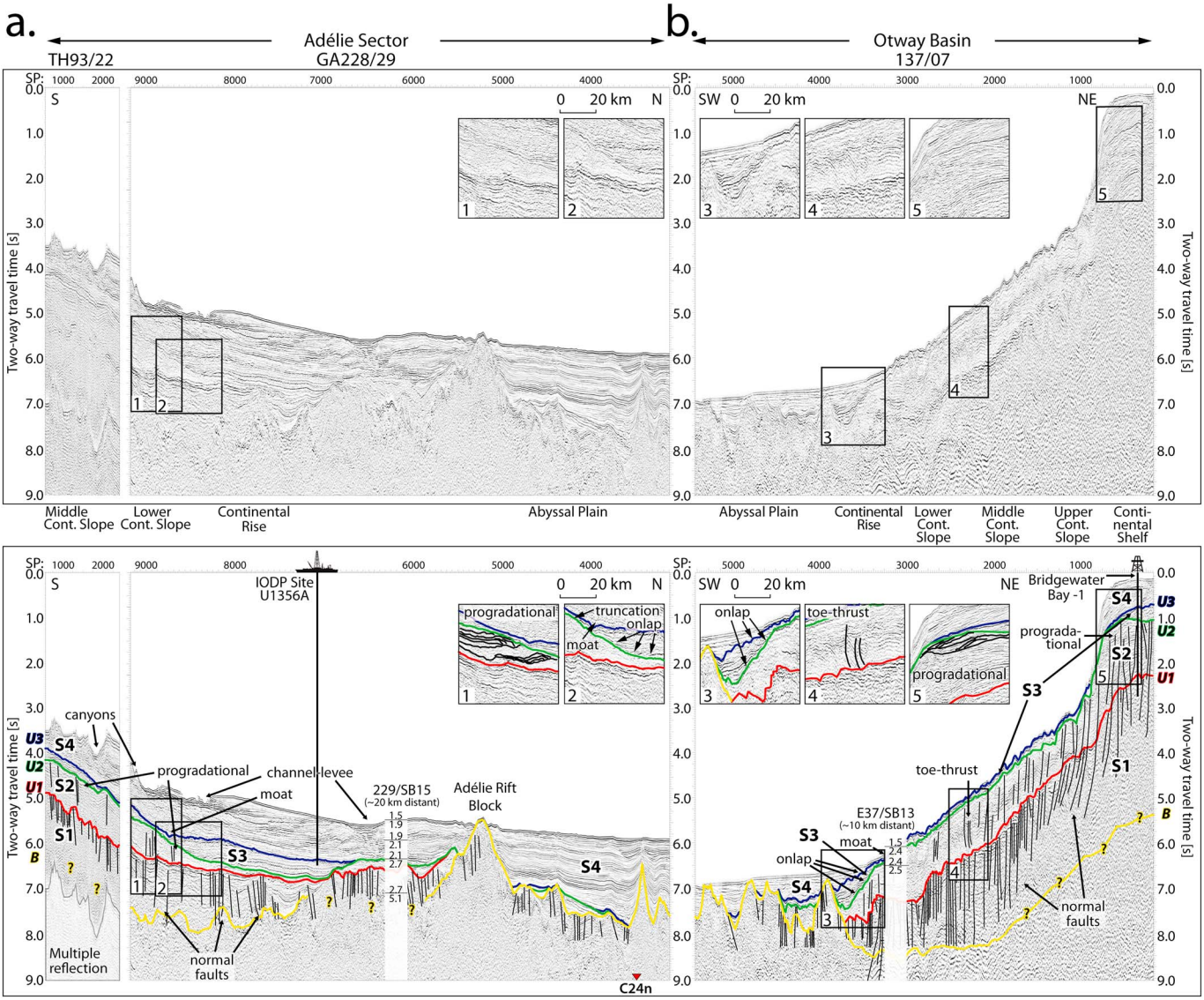

Figure 6. Uninterpreted (top) and interpreted (bottom) conjugate seismic reflection profiles offshore (a) Antarctica and (b) Australia in the eastern Australian-Antarctic Basin (location, see Figure 1a). Legend as in Figure 4. A high-resolution (1,200 ppi) version of this figure can be found in the supporting information (S3).

preglacial sediments on the Antarctic margin (Eocene, <54 Ma, Tauxe et al., 2012). Piston cores (Figure 1a) recovered Eocene/Paleocene shelf material (Sabrina Coast Sector; Gulick et al., 2017) and Cretaceous shelf sediments (George V Sector; Domack et al., 1980). However, both locations cannot be directly correlated to the seismic stratigraphy of the continental slope, due to the lack of seismic profiles in this area at the time of this study.

Along the southern Australian margin, key geological data are obtained from scientific drilling: ODP Leg 182 (Eyre Subbasin; Feary et al., 2000), ODP Leg 189 (offshore Tasmania; Exon et al., 2001), and DSDP Leg 29 (offshore Tasmania; Kennett et al., 1974). Further constraints are obtained from 15 industry wells: Jerboa-1 (Eyre Subbasin); Eucla-1 and Eyre-1 (onshore Eucla Basin); Platypus-1, Potoroo-1, Greenly-1, Borda-1, Gnarlyknots 1, and 1A (Ceduna Subbasin); Echidna-1, Duntroon-1, and Vivonne-1 (Duntroon Subbasin); and Morum-1, Amrit-1, and Somerset-1 (Otway Basin). A biostratigraphic summary of the well sites in the GAB is provided by Morgan et al. (1995). Additional geological information from the continental slope is provided by dredge samples collected in the GAB (BMR Survey 66; Davies et al., 1989). In the Bremer Subbasin, dredge samples were collected along deep-cutting canyons (Survey 265; Monteil et al., 2005).

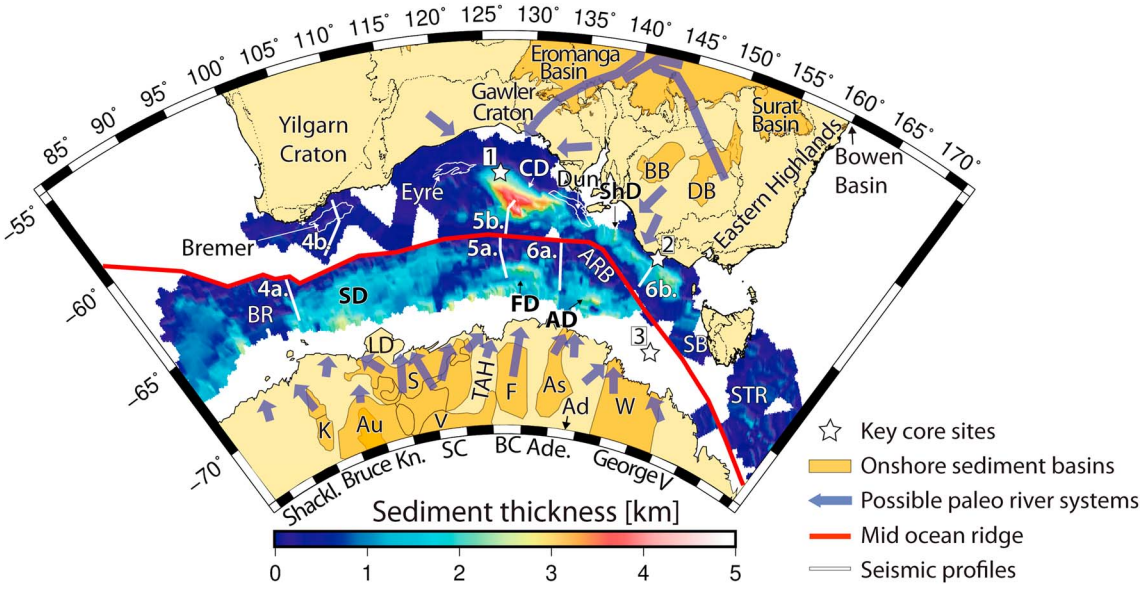

Figure 7. Isopach map of sedimentary unit S2, deposited during the Late Cretaceous. Possible paleoriver systems are shown as blue arrows (central Australia—after Lloyd et al., 2016; eastern Australia—after Gingele & De Deckker, 2005; Antarctica—this study; interpretation follows present-day ice flow directions after Jamieson & Sugden, 2008). Main depocenters are the Ceduna (CD), Sherbrook (ShD), Sabrina (SD), Frost (FD), and Astrolabe Delta (AD). Legend is shown in the figure. ARB = Adélie Rift Block, BB = Berri Basin, BR = Bruce Rise, DB = Darling Basin, Dun = Duntroon Subbasin, LD = Law Dome, SB = Sorell Basin, STR = South Tasman Rise, TAH = Terre Adélie Highlands. Legend for subglacial sediment basins and Antarctic sectors, see Figure 1c and Ad = Adventure Trough, Au = Aurora, V = Vincennes. Key geological sites are (1) Potoroo-1, (2) Bridgewater Bay-1, and (3) Piston-Core Site DF79-38. Time of reconstruction is 67 Ma, using the plate model of Whittaker, Williams, et al. (2013).

3.4. Magnetic Isochrons

Key seismic horizons more distant from the slope onlap onto oceanic crust, which provides constraints on their maximum depositional age, as sediment can only be deposited onto oceanic crust that has already formed. For this age correlation, we use magnetic anomaly identifications by Tikku and Cande (1999) and Whittaker et al. (2007).

For consistency, all ages determined from seafloor spreading anomalies and geological data were converted to the GTS2012 timescale (Gradstein et al., 2012; Figure 2), where possible.

4. Results and Interpretation

As the Australian and Antarctic margins share a similar tectonic, and likely climatic, evolution from initial rifting until the Eocene/Oligocene icehouse transition (plate tectonic reconstructions; see Figures 7 and 9), strong similarities can be observed in structural patterns, seismic characteristics, and boundary horizons of the sedimentary units. Here we develop a consistent seismostratigraphic framework and identify/interpret four major sedimentary units (S1–S4; Figures 4–6) and three key horizons (U1–U3) along both conjugate margins.

4.1. Sedimentary Unit S1

S1 is the oldest sedimentary unit that can be consistently observed along both margins. Extensive high-angle normal fault structures are most characteristic (Figures 4–6, black lines) and control extensional depocenters across the basins of both margins. Widespread and large-scale gravity-driven growth faults can be observed, particularly in the central GAB (Figure 5b). These structures have been described in detail, by, for example, Totterdell et al. (2000). At some locations, truncations of internal reflections are detected within S1, indicative of the locally complex structural and depositional history encompassed in this succession (Figure 4b, Bremer Subbasin).

The top boundary of this unit is a prominent high-amplitude reflection that can be easily detected along both margins (Figures 4–6, red horizon U1). U1 marks the top of the extensive faulting (Figures 4–6). Only some

faults in the GAB progress into sequence S2 but show a different direction pattern, indicating that they have been reactivated (see section 4.2). In some locations, U1 forms the top of the truncation of the underlying S1 (Figure 4b (5)). In most seismic profiles, the resolution in the deeper sections does not allow consistent detection of the lower boundary of S1, the crustal basement reflection (Figures 4–6, yellow horizon B). At locations where the basement can be identified, fault structures are observed extending through S1 into the basement (Figure 4b, Bremer Subbasin). Due to the difficulty in interpreting the basement, the S1 thickness cannot be determined based on the seismic reflection profiles.

Along the southern Australian margin, horizon U1 is dated as Late Santonian (~83 Ma, based on spore-pollen and dinocyst biozonation; Totterdell et al., 2000) in its central and eastern part (Ceduna, Eyre, Duntroon Subbasins, and Otway Basin; Figure 2). In the Sorell Basin, U1 is early Campanian (~80 Ma, based on spore-pollen biozonation; Stacey et al., 2013; Figure 2). In the Bremer Basin, dredge samples recovered slightly older material immediately below U1, which are dated to Cenomanian (~94 Ma, based on dinoflagellate biozonation; Monteil et al., 2005; Mantle et al., 2009; Figure 2). However, possible incomplete sampling with dredging may cause an inherent uncertainty for age estimates. Along the Antarctic conjugate, no drill sites have penetrated material of similar age. However, previous studies (e.g., Close et al., 2009; Eittreim et al., 1995; Leitchenkov et al., 2007, 2012; Wannesson et al., 1985) inferred a Turonian age for horizon U1 due to the perceived seismic similarities to the Australian margin, but which is slightly older than the GAB dating (Figure 3). Sedimentary unit S1 on both margins underlying U1 is widely agreed upon to have been deposited during the long-lasting rifting phase between Australia and Antarctica since the Middle-Late Jurassic. In the central and western Australian margin, the oldest S1 sediment overlying the basement is dated to Callovian-Kimmeridgian (~165 Ma, based on spore-pollen biozonation; Monteil et al., 2005). In the Otway Basin, the oldest dated material is of Valanginian age (~140 Ma, spore-pollen biozonation), with the basal, undrilled sediments likely to be Berriasian or older (Krassay et al., 2004).

Our interpretation of horizon U1 conforms with previous studies on the Australian margins (Monteil et al., 2005; Stacey et al., 2013; Totterdell et al., 2000). As the age can be determined directly on sediment samples, we infer the same ages (Figures 2 and 3). As no drill sites provide U1 age constraints for the Antarctic margin, we imply the Australian U1 ages directly to the Antarctic conjugate leading to a slightly different U1 age determination compared to previous studies (Figure 3). We determine an U1 age of ~94 Ma in the west (Bruce and Knox sectors), ~83 Ma in the center (Sabrina Coast, Banzare Coast, and Adélie sectors), and ~80 Ma in the east (George V Sector). For the western part of the Antarctic margin (Figure 4a), our U1 interpretation varies from Close et al.s (2007) tur horizon (1-s TWT shallower). However, the inclusion of newly available margin-parallel tie profiles provides high confidence in our stratigraphic correlation.

4.2. Sedimentary Unit S2

Unit S2 exhibits a complex internal structure. In most places, fault structures extend through the entire S2 unit (Figures 4a, 5b, and 6, black lines). Particularly in the central GAB (Figure 5b), many of these faults originate from underlying fault systems in S1 but follow a slightly different pattern, indicating that they have been selectively reactivated. After Totterdell and Krassay (2003b), Maastrichtian-early Paleocene flexure of the margin caused this reactivation process. Additionally, distinctive fault systems and partial décollement surfaces are visible (Figure 5b (5)), and, in places, toe-thrust structures are present on the lowermost slope (Figures 5b (3) and 6b (4)). In most parts of the margins, S2 is also characterized by a progradational architecture (Figures 5b and 6). On the western portion of the Australian margin, where S2 is markedly thinner (<0.6 km; Figure 7), faults and progradational geometries are less common. Here internal reflections are continuous and typically subparallel to the underlying topography (Figure 4b).

Horizon U1 represents the lower boundary of S2. Toward the abyssal plain along both margins, sedimentary unit S2's internal reflections become more flat-lying and pinch out onto the underlying basement (yellow horizon; Figures 4a, 5, and 6a). The top boundary of S2, horizon U2, is a prominent high-amplitude reflection (Figures 4–6, green horizon) that marks the top of the fault structures in the central and eastern sector of the margins, which are particularly prominent along the Australian margin. Across the shelves in the central sector, U2 forms a characteristic angular unconformity (Figure 5b). Farther basinward and particularly in the west, U2 is a prominent disconformity with high amplitudes (Figures 4a and 4b). On the lower continental slope, U2 can be easily detected by the onlapping pattern of the overlying internal reflections of

sedimentary unit S3 (Figures 5 and 6) and by truncation of underlying S2 reflections in the middle continental slope (Figures 5 and 6a).

The thickness of sedimentary unit S2 varies significantly along both margins (Figure 7). Offshore Australia, S2 is thickest in the Ceduna, eastern Recherche, and outer Duntroon subbasins, as well as in the Otway Basin (Figure 7, up to 5 km). Offshore Antarctica, thickest S2 deposition is observed offshore the Sabrina, Frost, and Astrolabe subglacial sediment basins (Figure 7, up to 3 km). In contrast, S2 is very thin or entirely absent in the Australian Eyre and inner Duntroon subbasins as well as on top of the Antarctic Adélie Rift Block and Bruce Rise (Figure 7).

Our interpretation of horizon U2 is identical to previous interpretations along the Australian margin (Figures 2 and 3). Ceduna Subbasin drill sites record an early-middle Paleocene hiatus between ~65 and 59 Ma, which is correlated to U2 (based on spore-pollen and foraminifera biozonation; Totterdell et al., 2000). In the Bremer Subbasin, numerous dredge samples did not recover any material datable to ~65–59 Ma, which indicates that a similar hiatus is present in this region (based on dinoflagellate biozonation; Monteil et al., 2005). Drill sites in the adjacent Eyre and Inner Duntroon subbasins reveal that sedimentary unit S2 is absent leading to the merging of horizons U1 and U2, corresponding to a break in the stratigraphic record of ~24 Myr (~83–59 Ma, based on spore-pollen and foraminifera biozonation; Totterdell et al., 2000; Figure 2). In the Otway and Sorell basins, U2 is dated by drill sites to latest Maastrichtian-early Paleocene (~65 Ma; based on spore-pollen biozonation; Krassay et al., 2004; Boreham et al., 2002; ~67 Ma onshore in the Otway Basin; Frieling et al., 2018; Figure 2). Consequently, sedimentary unit S2 was likely deposited between ~94 and 65 Ma in the Bremer Subbasin, ~83 and 65 Ma in the central Ceduna, eastern Recherche, outer Duntroon subbasins, and offshore the Otway Basin, and ~80 and 65 Ma in the Sorell Basin. S2 is not present in the Eyre and Inner Duntroon subbasins.

On the Antarctic margin, the age and stratigraphic interpretation of horizon U2 varies between previous studies (Figure 3), as no drill sites have penetrated U2 or S2. Our interpreted horizon U2 is most similar to the Antarctic horizon "$WL1_3$"/"WL2" interpreted by Leitchenkov et al. (2007, 2012), who determined U2 as a 67 Ma "Otway Basin breakup unconformity" and extended the interpretation along the Wilkes Land margin. They suggest a depositional age for sedimentary unit S2 of ~67–43 Ma. Here we make a slightly different comparison to the U1 and U2 age determinations published for the Australian margin and suggest that S2 along Antarctica was deposited from ~94 to 65 Ma in the Bruce, Knox sectors (similar to the Bremer Subbasin); from ~83 to 65 Ma in the Sabrina Coast, Banzare Coast, Adélie, and western George V sectors (similar to the conjugate Ceduna Subbasin and Otway Basin); and from ~80 to 65 Ma in the eastern George V Sector (similar to the Sorell Basin). On top of the Adélie Rift Block and Bruce Rise, S2 is very thin or entirely absent, similar to the Eyre and the inner Duntroon subbasins (Figures 2 and 7).

4.3. Sedimentary Unit S3

Unit S3 represents a shorter time span and is significantly thinner than the underlying sedimentary units on both conjugate margins. The top and lower boundaries, horizons U3 (blue) and U2 (green), merge into one reflection band and/or a very thin layer beneath the middle continental slope and diverge again toward the upper slope and toward the base of the continental slope (Figures 4–6 and 9). This means that sedimentary unit S3 is split into two main locations, one thinner deposit along the middle continental slope (maximum ~0.7 km) and one thicker deposit along the continental rise (maximum ~1.2 km).

Along the base of the continental slopes in the center and east, the internal reflections of S3 onlap onto the lower boundary U2 (Figures 4–6). The top boundary is the high-amplitude horizon U3, which is also the uppermost reflection onlapping onto older layers (Figures 4–6). At the central and eastern continental rise along both margins (Figures 5 and 6, zoom-ins), horizon U3 is easily detectable by onlapping internal reflections of overlying sedimentary unit S4 onto U3. In the western part of the Australian-Antarctic margins (Figure 4), both boundary horizons U2 and U3 are mostly subparallel to the overlying S4 reflections and the seafloor.

Along the Australian shelves, our interpretation of horizon U3 is identical to previous studies (Figures 2 and 3). U3 is dated to ~50 Ma in the western Bremer Subbasin (based on dinoflagellate biozonation; Monteil et al., 2005), ~48 Ma in the central Eyre, Ceduna, and Duntroon subbasins (based on foram and spore-pollen biozonation; Totterdell et al., 2000), and ~45 Ma in the eastern Otway and Sorell basins

(based on spore-pollen biozonation; Krassay et al., 2004). Therefore, on the Australian shelves, S3 was deposited between ~59 and 50 Ma (Bremer Subbasin), ~59 and 48 Ma (central GAB), and ~65 and 45 Ma (Otway, Sorell basins). Dredge samples from the eastern GAB's continental rise recovered early-middle Eocene age material (~54–44 Ma) from the continental rise's S3 (based on nannofossil biozonation; Shafik, 1992; Figure 9). On the Antarctic margin, our U3 interpretation corresponds to the Eocene hiatus, from ~47.9 to 33.6 Ma, observed in IODP site U1356 (based on dinoflagellate and nannofossil biozonation; Tauxe et al., 2012). The older age of this hiatus is similar to the constraints from the central part of the Australian conjugate. At U1356, a second hiatus (~51.9–51.06 Ma) follows directly below U3 (~70 m), which we interpret to be imaged by an internal reflection of S3.

Along the Antarctic margin, significant differences exist between our horizon U3 interpretation and previous studies (Figure 3). Leitchenkov and Guseva (2012) defines two horizons ("WL3" ~ 42/43 Ma; "WL4" ~34 Ma), which merge to one horizon in the Adélie Sector (this study: U3, close to IODP Site U1356). In most places, particularly in the Sabrina and Banzare Coast sectors, Leitchenkov and Guseva (2012)'s "WL4" interpretation follows a reflection that we interpret as an internal reflection of the younger S4 unit, due to the prominent channel-levee structures (see section 4.4). From the Bruce to the Banzare Coast sectors, our interpretation of U3 is identical to the "eoc" (~45 Ma) horizon interpreted by Close et al. (2007). However, in the Adélie Sector, "eoc" is located much deeper than the drilled Eocene unconformity (U1356) and is equivalent to our horizon U2.

In the central GAB, Totterdell et al. (2000) interpreted that the S3 sediments at the continental rise were deposited around the same time as the shelf unit. We propose that a similar sedimentation pattern also existed along other parts of the Australian margin and offshore Antarctica, based on strong seismic similarities. On both upper slopes and shelves (Figures 4–6), sedimentary unit S3 is a thin wedge-shaped drape containing subparallel internal reflections with medium to high amplitudes (Figures 4b, 5b, and 6).

The continental rise deposits on both margins also share similarities in overall morphology and internal seismic characteristics (Figure 8). Here we interpret these features as extensive contourite drift deposits (after Rebesco et al., 2014). Our interpretation is based on combining evidence from characteristic seismic structures, S3's shape and thickness, sedimentary records, and regional oceanographic context (detailed discussion, see sections 5.2 and 5.3). As the term "contourites" has been used differently in previous studies, we follow the definition "sediments deposited or substantially reworked by the persistent action of bottom currents" (after, e.g., Stow et al., 2002; Rebesco et al., 2014).

The following continental rise S3 structures are observed and interpreted:

1. Mounded drifts: At the continental rise, where the underlying topography is steeper, S3 forms elongated, slightly asymmetric, mounded features that thin toward the abyssal plain (Figures 5b, 8a, 8e, and 8f). These deposits show significant variations in amplitudes and contain layers with more chaotic reflection patterns, onlapping onto the lower boundary reflection.
2. Channel-related drift: Within the narrow pathway between the Adélie Rift Block and the Antarctic continental slope, the sediment formed a mounded "channel-related drift" (Figure 6a/8d). Internal reflections are similar to the mounded drifts; however, they onlap onto the lower boundary reflection at both ends.
3. Mixed drifts: Some of the mounded drifts show characteristics of "mixed drifts" with increases in chaotic internal reflections and partly rotated blocks, which indicate structural appearance of debris flows (Figure 8g) or slumps (Figure 8h). These drifts are observed in the eastern part of both margins, downslope of the Eyre and Duntroon subbasins (Figure 9), as well as near locations on both margins where S2 internal reflections truncate in a large scale onto horizon U2 farther upslope, indicating possible erosion followed by redeposition as "mixed drifts" downslope (Figure 8c). These interpreted contourites are mixed with downslope mass transport deposits.
4. Sheeted drifts: Areas where the underlying topography is gentler, S3 thins and forms widespread sheeted layers from the midslope into the abyssal plain (Figures 4a, 5a, and 8b). Internal reflections are mostly subparallel and high amplitude.

In the central GAB, an elongated S3 unit containing both mounded and mixed drifts extends along the continental rise for more than 950 km and about 130 km seaward, reaching ~1.2-km thickness (Figures 5b and 9). Along the Antarctic conjugate, an elongated mound at the continental rise at the

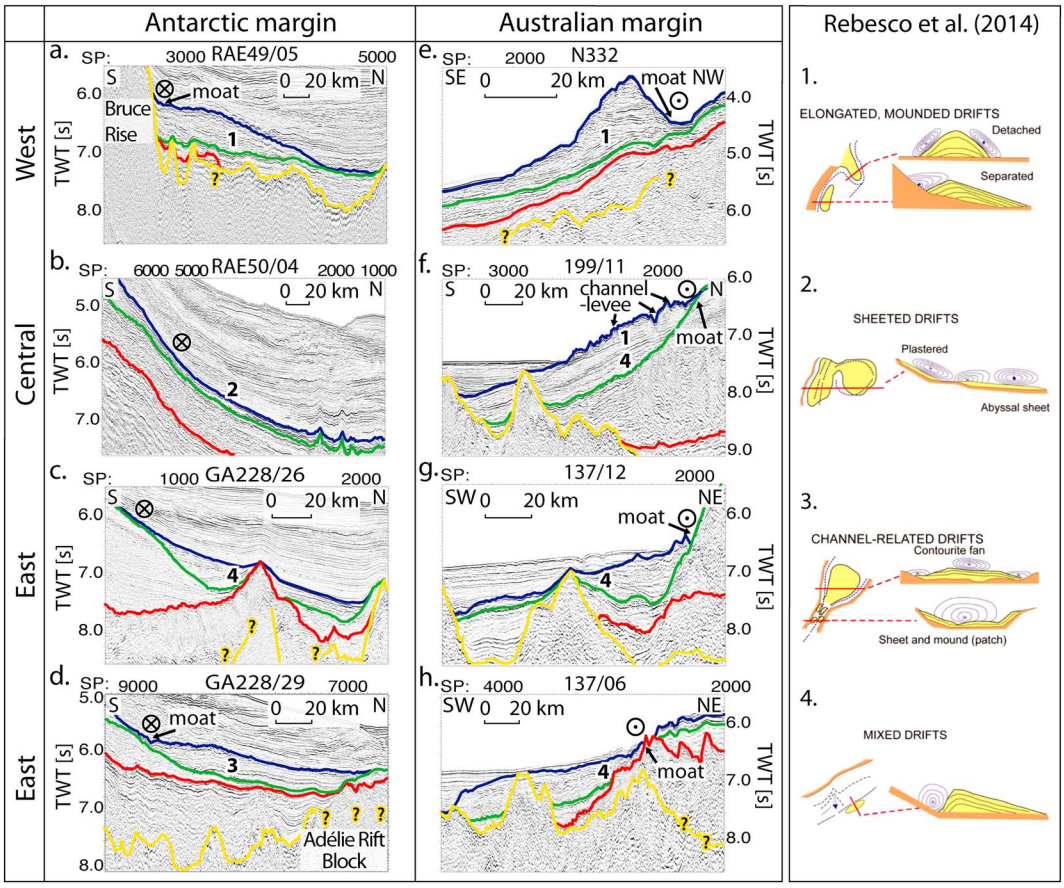

Figure 8. Key examples of observed contourite drift deposits along the Antarctic (left, a–d) and Australian (middle, e–h) margins. The types of drifts observed in this region are shown in the right column (Rebesco et al., 2014; after Stow, Kahler, & Reeder, 2002) and determined in the (a–h). A high-resolution (1,200 ppi) version of this figure can be found in the supporting information (S4).

Bruce Rise reaches ~0.9-km thickness and extends about 400 km margin-parallel and 110 km seaward (Figures 8a and 9).

The "channel-related drift" between Adélie Rift Block and continental slope extends about 400 km and fills up the depression with about 0.8 km of sediment over widths up to 130 km (Figures 6a, 8d, and 9). The "mixed drifts" extend through the Otway and Sorell basins (~550 km; Figures 6b, 8g, and 8h) as well as in the Adélie and George V sectors of the Antarctic conjugate (~300 km). They extend about 140 km offshore, similar to the mounded drifts, and reach thickness up to 1.2 km.

"Sheeted drifts" are interpreted along the midslope to abyssal plain in the Antarctic Knox, Sabrina Coast, and George V sectors (Figures 4a, 5a, 8b, and 9). They extend much farther toward the ocean than the mounded drifts (about 250–350 km); however, they only reach a thickness of about 300 m.

4.4. Sedimentary Unit S4

The uppermost sedimentary unit S4 overlies horizon U3 and shows strong differences between Australia and Antarctica. Along the Australian margin, this unit is very thin (~0–1 km thick; Figure 10) and consists of parallel, mostly continuous high-amplitude reflections forming a wedge-shaped drape along the shelves and upper slopes (Figures 4b–6b). This leads to exposure of underlying sedimentary units S3 and S2 along the middle continental slope offshore Australia. Hemipelagic sedimentation in the abyssal plains shows mostly subhorizontal layering with medium to high amplitudes (Figures 4b–6b).

In contrast, S4 shows complex internal structural variations along the Antarctic margin, including numerous mostly asymmetric channel-levee systems with continuous internal reflections and filling strata in the channels (Figures 4a (1) and 6a), progradating features, and undulating sediment waves in the uppermost

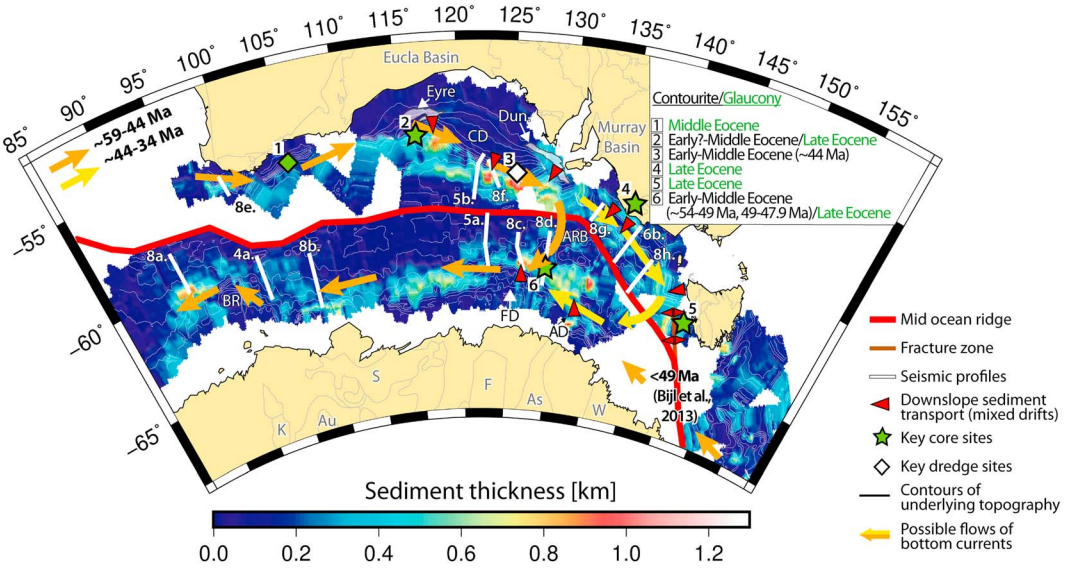

Figure 9. Isopach map of sedimentary unit S3, deposited during the Paleocene/early Eocene. Arrows indicate clockwise flowing ocean currents progressing eastward (legend, see figure). Red arrows show downslope sediment transport sourcing the contouritic drifts. Green stars show drill and dredge locations with Eocene glauconite occurrence. Geological age constraints of contourite (black) and glauconite (green) formation are shown in the figure. Key geological sites are (1) Dredge Survey 265, (2) ODP 1128, (3) Dredge Survey 66-102DR07, (4) sediment samples onshore (Houben et al., 2019), (5) ODP 1168, and (6) IODP U1356. Legend for subglacial sediment basins, see Figure 1c. Time of reconstruction is 43.8 Ma, using the plate model of Whittaker, Williams, et al. (2013).

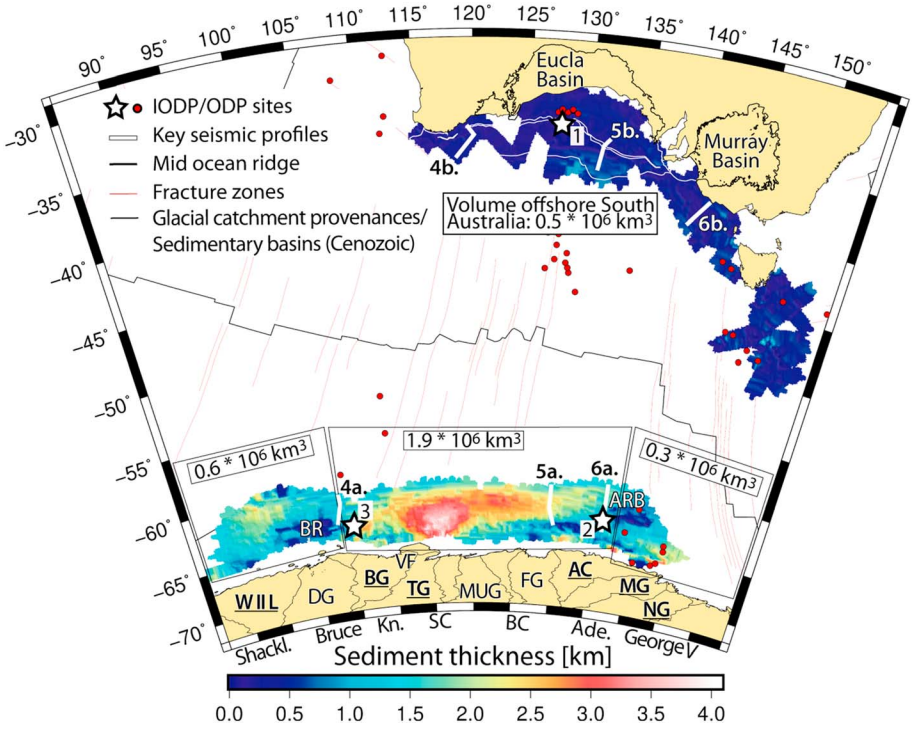

Figure 10. Isopach map of sedimentary unit S4, deposited post-Eocene. Offshore Antarctica, thick glacial sediment units are deposited, particularly offshore the Vanderford (VF), Totten, Mertz, and Ninnis glaciers (underlined). Glacial catchment provenances (Fretwell et al., 2012) are shown: WIIL = Wilhelm II Land, DG = Denman Glacier, BG = Bond Glacier, VF = Vanderford Glacier, TG = Totten Glacier, MUG = Moscow University Glacier, FG = Frost Glacier, AC = Adélie Coast, MG = Mertz Glacier, NG = Ninnis Glacier. The Cenozoic sedimentary basins are shown after Totterdell and Bradshaw (2004). The calculated sediment volumes and the legend are shown in the figure. ARB = Adélie Rift Block, BR = Bruce Rise. Key drill sites are (1) ODP 1128, (2) IODP Leg 318, (3) and ODP 268.

parts (Figure 4a (4)). Particularly in the central Antarctic sectors, the reflections onlap prominently onto U3 and show subhorizontal structure with high amplitudes (Figure 5a).

The thickness of S4 is variable along the Antarctic margin, reaching up to 4 km proximal to the Totten Glacier in the Sabrina Coast Sector and ~2.5 km in the George V and Shackleton sectors (Figure 10). In contrast, at parts of the Adélie Sector, S4 is less than 0.5 km thick (Figure 10) with deep cutting canyons (Figure 6a). Drill sites offshore Antarctica recovered glaciogenic sediment deposits from unit S4, which have been studied in detail by various authors (e.g., De Santis et al., 2003; Donda et al., 2007; Escutia et al., 2002, 2003, 2005).

Along the Australian shelves, S4 is younger than ~50 Ma in the western part (based on nannofossil and foraminifera biozonation; Feary et al., 2000), ~48 Ma in the central part (based on spore-pollen biozonation; Totterdell et al., 2000), and ~45 Ma in the eastern part (based on spore-pollen biozonation; Krassay et al., 2004; Figure 2). Along most of the middle continental slopes offshore Southern Australia, S4 is very thin or absent (Figures 4–6). No direct age constraints exist for the hemipelagic S4 deposit in the Australian abyssal plains; however, it may have a similar oldest age as S4 respective to their shelves. In the Antarctic Adélie Sector, the lower boundary of glacial unit S4 is dated to ~33.6 Ma (based on dinoflagellate biozonation; Tauxe et al., 2012). Younger parts of this unit are drilled at numerous places (e.g., IODP Leg 318 and ODP Leg 28; see Houben et al., 2013).

Previous studies offshore Antarctica subdivided the uppermost glacial sediment package into subunits (3, Leitchenkov et al., 2007; 6, De Santis et al., 2003). As no glacial deposition occurred offshore Australia, we combine these subunits to one sedimentary unit S4.

5. Discussion

5.1. Late Cretaceous Deltaic Sedimentation

Offshore Australia, sedimentary unit S2 is well recognized to have been sourced by fluvial drainage systems, with a depositional environment changing from inboard fluvial, through delta plain and prodelta, to marine setting (e.g., Hammerhead Supersequence; after Totterdell et al., 2000). Numerous drill sites offshore southern Australia have recovered thick layers of sand-rich deltaic material deposited during the Late Cretaceous due to terrigenous influx from large paleoriver systems (e.g., Feary et al., 2000; King & Mee, 2004; Krassay & Totterdell, 2003; MacDonald et al., 2010; Totterdell et al., 2000; Totterdell & Krassay, 2003a). In the central GAB, S2 reaches thicknesses up to 5 km and a volume of ~0.29×10^6 km^3, as part of the Ceduna Delta (e.g., Totterdell et al., 2000; Figure 7).

Although the Antarctic conjugate S2 does not reach the same thickness and extent as the Ceduna Delta, some similarities in reflection characteristics and sediment architecture can be clearly detected. We propose that a similar fluvial sediment mechanism was also active in Antarctica, with onshore paleoriver systems transporting sediment from interior basins into offshore depocenters. This interpretation is supported by Cretaceous sediments recovered with a piston-corer on the eastern Antarctic shelf which are characterized as fluvial material similar to the Australian margin (Figure 7; Site DF79-38; Domack et al., 1980).

Additionally, the Late Cretaceous climatic and tectonic setting of the nascent Australian-Antarctic Basin is realistic for such a depositional environment along both margins. Throughout the overall warm Late Cretaceous, the equator-to-pole temperature gradient was extremely low (e.g., Huber et al., 1995), and mean global precipitation rates were double those of the present day (Hay & DeConto, 1999). During this time, the Australian-Antarctic Basin was still very narrow (max. ~330 km; Whittaker et al., 2007), and it is probable that paleoclimatic conditions prevailing in Australia were similar in Antarctica.

In the Australian case, river systems were able to transport sediments over a long distance into the offshore basins. The paleo Ceduna river system feeding the Ceduna Delta had a catchment region extending to areas more than 1,000 km away (e.g., Raza et al., 2009; Veevers, 2001). Various authors have proposed that uplift of the Eastern Highlands from 100 to 80 Ma resulted in erosion of parts of the Bowen and Surat basins in eastern Australia and transport of this material to the Ceduna Subbasin (Raza et al., 2009; Totterdell & Krassay, 2003b; Veevers, 2001; Figure 7). Another prominent delta, the Sherbrook Delta (Blevin & Cathro, 2008), is observed in the Otway Basin and was possibly fed with material eroded from the onshore Darling Basin (after Gingele & De Deckker, 2005; Figure 7). In contrast, not much sediment is deposited

offshore in regions that are not connected to large drainage systems and eroding hinterlands. For instance, lower rates of denudation on the Yilgarn Craton in western Australia might be a cause for limited deltaic sedimentation in the Bremer Subbasin (Figure 7). In the Eyre and inner Duntroon subbasins, possible uplift-related erosion in the Late Cretaceous resulted in the absence of S2 (Krassay & Totterdell, 2003; Totterdell et al., 2000; Totterdell et al., 2014). At the South Tasman Rise and eastern Sorell Basin, oblique extension associated with a developing transform part formed small, isolated depocenters during the Late Cretaceous, which likely led to less accumulation space for deltaic material (Stacey et al., 2013).

Ancient river systems and their catchment areas are difficult to map in Antarctica because of the thick ice sheets. However, our study shows that main deposition centers along the Antarctic margin are located offshore the Sabrina, Frost, and Astrolabe subglacial sediment basins (terminology after Aitken et al., 2014; Figure 7) and reach thicknesses up to 3.0 km. Possible paleoriver catchment areas may have covered the coastal sediment basins (e.g., Sabrina, Frost, and Astrolabe) or, similar to the Australian conjugate, extend farther inland to, for example, the Aurora and Vincennes sediment basins in the west and/or the Adventure Subglacial Trough or parts of the Wilkes sediment basin in the east (Figure 7). Aitken et al. (2016) and Gulick et al. (2017) argue for large-scale erosion of the Sabrina sediment basin during repeated advance and retreat of the East Antarctic Ice Sheet throughout glacial-interglacial cycles since the Oligocene. We suggest that this region possibly experienced significant erosion by large river systems already in the Late Cretaceous.

Previous studies (e.g., Cooper et al., 2001; Jamieson et al., 2005, 2010; Jamieson & Sugden, 2008) propose that established preglacial paleotopographic structures were retained by the evolving ice sheet and resulted in the present-day subglacial drainage systems. This means in turn that present-day glacial systems to a large extent reflect ancient river catchment areas. Our interpretation of possible paleoriver systems (Figure 7, blue arrows, Antarctic side) follows the reconstruction of present-day subglacial drainage patterns by Jamieson and Sugden (2008). In particular, the modern Vanderford, Totten, Frost, and Mertz Glacier drainage systems (Figure 10; after Fretwell et al., 2012) might have been large river beds feeding the thick offshore delta deposits during the Late Cretaceous. In contrast, the eastern part of the Sabrina Coast Sector shows a thin S2 layer (<1 km), which could be related to lower denudation rates on the onshore Terre Adélie Highlands (Figure 7).

5.2. Sedimentary Unit S3 Contourites

On the Australian margin, previous studies interpreted the continental rise portion of unit S3 as mass transport deposits (Wobbegong Supersequence; Totterdell et al., 2000). On the Antarctic conjugate, Close (2010) described these features as "healed-slope and/or ponded deposits." Leitchenkov et al. (2015) interpreted some of these features around the Bruce Rise (Figure 8a) as contourite deposits formed by a westward flowing ocean current.

We interpret extensive contourite drifts on both continental rises as part of S3. The criteria used to determine contourite drifts, and particularly to distinguish them from turbidites, are highly debated in the literature (e.g., Hüneke & Stow, 2008; Rebesco et al., 2014; Shanmugam, 2000, 2017). Here we combine evidence from characteristic seismic structures, thickness, and shape of Sedimentary Unit S3, with characteristic features found in sediment samples and the regional oceanographic context of the basin, and conclude that the presence of contourites is most likely.

Contourites form due to long-slope bottom current activity (terminology after Stow, Faugères, et al., 2002; Rebesco et al., 2014) and vary significantly in their shape, depending on the underlying topography, sediment supply, and ocean current activity (e.g., Rebesco et al., 2014). Ocean currents speed up along steeper slopes and narrow pathways, eroding and redepositing sediment as "mounded drifts." Contourite drifts transform into "sheeted drift" deposits (Figure 8b) when the slope angle is gentler and bottom currents affect a broader region, possibly slow down, and erosion is nonfocused (e.g., Faugères & Stow, 2008; Rebesco et al., 2014). The "mixed drifts" with partly internally rotated blocks are contourite drifts influenced by additional downslope movements (e.g., Mutti & Carminatti, 2011; Rebesco et al., 2014), for example, possibly by debris flows (Figure 8g) or slumps (Figure 8h).

Geological characteristics that have been interpreted by numerous researchers to be typical of contouritic formations include contorted, convoluted bedding, interbeds, fining-/coarsening-upward sequences (grain size distribution is dependent on current speed; for example, Rebesco et al., 2014; Stow & Lovell, 1979; Stow et al., 2002). Contrary to purely downslope turbidite deposits, contourites are deposited over much

longer timescales, with lower sedimentation rates and extensive bioturbation (e.g., Rebesco et al., 2014; Stow & Faugères, 2008). Contourite drifts usually contain reworked microfossils.

Our interpretation of contourites is supported by drill and dredge samples on both margins. Reworked Late Cretaceous microfossil material is detected in Eocene assemblages along the entire southern Australian margin (Figure 9), including dinoflagellates in the Bremer Subbasin (Bradshaw, 2005; Monteil et al., 2005) and nannofossils at the GAB's continental slope (Shafik, 1973, 1983, 1990, 1992). At the continental slope of the central GAB (Figure 9), ODP Site 1128 recovered early-middle Eocene sediment with extensive burrowing, bioturbation, low sedimentation rate (~4 m/Myr), and fining-upward sequences in the lowermost lithological unit (Feary et al., 2000).

On the Antarctic margin, at IODP Site U1356, evidence for contourite drifts exists, particularly in the upper part of sedimentary unit S3, including contorted and convoluted claystones, well stratified and clast-bearing sandstones, bioturbation, fining- and coarsening-upward sequences, relatively low sedimentation rate of about 24 m/Myr (Escutia et al., 2011; Tauxe et al., 2012). These lithological characteristics are less common in the deeper part of S3 (>49 Ma); nevertheless, Escutia et al. (2011) observed some bioturbation, "rare interbeds of massing or cross- and parallel-laminated fine sand- and siltstones," one interbed of 30-cm-thick layer of poorly sorted sandstone, and mica minerals that usually form during increased current activity (e.g., Rebesco & Camerlenghi, 2008; Stanley, 1993).

In some areas, the S3 unit is likely formed by a mixture of long-slope contouritic and down-slope turbiditic flows coming from the upper slopes and shelves, which we determine as "mixed drifts" (Figures 8c, 8g, and 8h). This is particularly the case toward the east along both margins, downslope of the Eyre and Duntroon subbasins on the Australian margin, and partly downslope locations where S2 internal reflections are truncated by the overlying U2 horizon (Figures 5 and 9; red arrows indicate downslope sediment transport). These truncations indicate gravitational instability of S2 due to its thickness (after Totterdell et al., 2000; Figures 8c and 8f). At locations where horizon U2 is a prominent angular unconformity or S2 is absent, possible Late Cretaceous uplift and erosion (after Totterdell et al., 2000) may have initiated downslope mass transport. These downslope-transported sediments were picked up by margin-parallel ocean currents and deposited as "mixed" contouritic deposits (Figure 9).

5.3. Clockwise Eocene Currents

We argue that the S3 contourite drifts were formed by currents circulating clockwise within the Australian-Antarctic Basin. The shape of the contourite drifts with respect to the continental slopes provides indications for the flow direction of the ocean currents forming them. The Coriolis force in the southern Hemisphere deflects along-slope ocean currents toward their left, leading to sediment erosion on their left (continental slope) and redeposition on their right (oceanward; Faugères & Stow, 1993). The contourite drifts detected in our seismic profiles along both margins are characterized by asymmetric mounds that thin seaward and internal reflections onlapping at the moat side (Figure 8). This indicates that the ocean currents forming the contourite drifts must have flown eastward along the Australian slope, most likely coming from the Indian Ocean, and westward along the Antarctic margin, forming a clockwise current system (Figure 9), as the Tasman Gateway was still closed during the deposition of this S3 unit (~58–48 Ma).

This interpretation is supported by geological observations and numerical modeling experiments along the Australian margin. At the eastern Ceduna continental slope (Figure 9), some dredged Late Cretaceous reworked nannofossils indicate that they have been eroded from sites farther west (Shafik, 1992) and redeposited during the middle Eocene, within a very narrow biostratigraphic interval (~43.5 Ma; Shafik, 1992). Based on these findings, Shafik (1992) proposed short-lived, easterly flowing bottom currents along the southern Australian margin. We suggest that most of the S3 sediments were eroded from older S2 sediments upslope, transported downslope, and redeposited as contouritic drifts farther eastward (westward) along the Australian (Antarctic) slope (Figure 9). This interpretation is supported by studies in the Otway Basin (Pollack, 2003), which suggest that the older deltaic material was remobilized by ocean currents and redeposited as "shoreface sands and barriers" via eastward longshore drift. On a broader scale, our observations are consistent with overall biogeographic patterns in dinoflagellate cysts showing influence of the low-latitude-derived Proto-Leeuwin Current on the Australian side of the basin, flowing east, and the westward flowing Proto-Antarctic Counter Current on the Antarctic Margin (Bijl et al., 2011; Bijl,

Sluijs, & Brinkhuis, 2013; Sijp et al., 2016). Considering that the Tasmanian Gateway was still very much restricted during the Eocene, these currents were most likely connected in a clockwise gyre.

It is possible that the clockwise ocean current circulation progressively extended farther east through the Eocene, which is supported by geological constraints offshore both margins. During the early Eocene, surface water temperatures were much warmer along the central and western part of the Australian margin compared to the eastern Otway Basin (based on nannofossil records; Shafik, 1990). This phenomenon has been explained due to an influx of warm water from the Indian Ocean into the Australian-Antarctic Basin, which did not reach the eastern sector at that time (Shafik, 1990). Farther east, around the South Tasman Rise and in the Sorell Basin (ODP Site 1168, 1170), the first evidence for ocean current activity is not observed until the late Eocene (Exon et al., 2001; Stickley et al., 2004).

There is evidence for strengthening ocean currents through the Eocene. We interpret this increase in current strength to have implications for the formation of unconformity U3 (details, see section 5.4). Nannofossil records along the Australian margin indicate an intermittent current flow with prominent phases of stronger flow in the middle and late Eocene, as well as in the middle Oligocene (Shafik, 1990). Along the Antarctic margin, conjugate to the eastern GAB, IODP Site U1356 reveals Eocene sedimentary structures (S3, see section 5.2) that support moderate strength and/or intermittent contourites operating prior to ~49 Ma, whereas after ~49 Ma, there is evidence for stronger and more continuous contourite formation. The onset of the westward flowing Antarctic Counter Current through the shallow Tasman Gateway (Bijl, Sluijs, & Brinkhuis, 2013) possibly amplified the clockwise ocean current speed.

The presence of glaucony minerals (products of cation exchange between seawater and sediment) is a strong indicator for moderately strong ocean currents (e.g., Amorosi, 1997; McRae, 1972; Odin & Fullagar, 1988; Odin & Matter, 1981; Rebesco & Camerlenghi, 2008). Along both margins, glauconite has been detected in Eocene shelf sediments (Houben et al., 2019; Sluijs et al., 2003; Figure 9). These glauconites suggest an increase in ocean current strength progressing from west to east. Glaucony has been observed in middle Eocene samples from the canyons of the Bremer Subbasin (Blevin, 2005; Bradshaw, 2005) and in early to late Eocene and younger rocks in the central GAB (Apollo-1 well site, Messent, 1998; ODP Site 1128, Feary et al., 2000). Late Eocene (~41–34 Ma) glauconites are detected around Tasmania (ODP Leg 189; Exon et al., 2001; Wei, 2004) and in reworked Oligocene material at IODP site U1356 (Houben et al., 2019).

The widening and deepening of the Australian-Antarctic Basin likely controlled the west to east progression and strengthening of clockwise ocean current circulation. The relationship between basin widening and ocean current strengthening is shown in ocean model simulations by Sijp et al. (2016). Nannofossil records indicate that the basin transformed from neritic (mainly middle shelf) to deeper marine environments from west to east, first in the GAB (~54–44 Ma) and later in the Otway Basin (~44 Ma–late Eocene; Shafik, 1983, 1990, 1992). The Sorell Basin and the South Tasman Rise were likely isolated by the Tasmanian-Antarctic Shear Zone (NW-SE direction), which probably acted as an oceanographic barrier, leading to anoxic to poorly ventilated conditions until the late Eocene (Exon et al., 2001; Figure 9).

Previous studies proposed a surface-water ocean current flowing clockwise in the Australian-Antarctic Basin during the Eocene—the Proto-Leeuwin Current (e.g., McGowran et al., 1997; Shafik, 1992; Stickley et al., 2004). Contourites can form in all water depths ("deep-water" (>2,000 m), "mid-water" (300–2,000 m), and "shallow-water" (<300 m) drift types; Stow, Kahler, & Reeder, 2002; Viana et al., 1998). Therefore, it is possible that the interpreted S3 contourites were formed by this strong gyre system. Model simulations suggest that the Australian-Antarctic Basin experienced the highest zonal velocities at the Australian side and particularly at shallower water depths (Sijp et al., 2016). Based on the ocean models (Sijp et al., 2016) showing increased gyre strength with widening of the Australian-Antarctic Basin and considering that the water column was likely to be less well stratified during the warmer Eocene, it is possible that the depth-integrated strength of the gyre may have affected the deeper seafloor. However, it is difficult to constrain with certainty whether the paleoseafloor was sufficiently shallow to be easily affected by surface current activity and/or if the Proto-Leeuwin Current was strong enough to affect deeper sections in the water column.

5.4. Formation of Horizon U3

Along the Australian margin, the establishment of an increasingly sediment-starved environment since the early Cenozoic strongly controlled the stratigraphic character of the sediments, including Horizon U3 (e.g.,

Bradshaw, 2005; Krassay et al., 2004; Totterdell et al., 2000; Totterdell et al., 2014). Along most of the Australian middle and lower continental slopes, a widescale exposure of old sediment units (early Eocene S3, Late Cretaceous S2, and older S1 rift sediment; Figures 4–6) is observed. We suggest that a drastic decrease in terrigenous sediment supply led to nondeposition at these parts of the margin. Our study shows similar sedimentary structures along the conjugate Antarctic margin, overlain by the thick post-Eocene glacial sedimentary unit S4. Based on this observation, we propose that the dominant driver for the formation of horizon U3 along the Antarctic slopes was nondeposition similar to the Australian conjugate, rather than erosional processes as proposed by previous authors (e.g., Close et al., 2007; Eittreim et al., 1995; Escutia et al., 2011; Leitchenkov & Guseva, 2012).

In general, we propose that two main processes dominated the formation of U3: decreasing terrigenous sediment supply offshore both margins and strengthening of the clockwise ocean currents in the deeper parts.

We suggest that a significant decrease in terrigenous sediment supply into the basin on both continents during the middle to late Eocene played a significant role forming horizon U3. Offshore southern Australia, a very thin drape of Cenozoic sediments (S3, S4) extends over large areas along the shelves and onshore. Previous studies described that a strong decrease in terrigenous sediment supply into the Australian basins occurred earlier, around 65 Ma (e.g., Bradshaw, 2005; Feary et al., 2000; Krassay et al., 2004; Totterdell et al., 2000; Totterdell et al., 2014). Benbow et al. (1995) proposed that Late Cretaceous-Paleocene uplift in the GAB's hinterland contributed to the reduction of sediment supply to the GAB (supported by Hall et al., 2016; Totterdell & Bradshaw, 2004). Progressive semi-aridification is affecting the hinterland due to the northward shifting of the continent into the subtropical zone and increasing warm water influx from the Indian Ocean intensified this terrigenous, clastic sediment cut-off from the middle Eocene (e.g., Feary et al., 2000), culminating in shelfal carbonate accumulation (S4) and along-slope nondeposition, which entirely lacked terrigenous, clastic material.

Antarctica may also have aridified during the late Eocene. After the early Eocene Climatic Optimum (<48 Ma), the global sea surface temperatures decreased progressively (e.g., Zachos et al., 2008), leading to the onset of glaciation in Antarctica with the first arrival of glaciers at the Wilkes Land coast around 33.6 Ma (e.g., Escutia et al., 2011). Evidence exists that some Antarctic glaciation had started to form prior to the Eocene/Oligocene-Transition (e.g., Anderson et al., 2011; Carter et al., 2017; Ehrmann & Mackensen, 1992; Gulick et al., 2017; Scher et al., 2014; Strand et al., 2003), particularly during the Priabonian oxygen isotope maximum "PrOM" event (37.34 and 37.19 Ma; Scher et al., 2014). Scher et al. (2014) noted that high-latitude cooling and formation of glaciers tend to strengthen the polar high-pressure regime and produce more arid conditions. This may have led to a decrease in fluvial runoff and less terrigenous influx into the basin as long as the glaciers do not reach the coast.

The previously discussed strengthening of ocean current activity through the Eocene likely culminated in winnowing, large-scale decreasing sediment accumulation, and eventually hiatus formation in the deeper parts of the basin (after Rebesco et al., 2014). The continuous global Cenozoic cooling (e.g., Zachos et al., 1994) may also have resulted in increasing strength of the thermohaline circulation and additional strengthening of the currents.

We do not discount that at least some sediment erosion occurred along the Antarctic shelves during the onset of glaciation around 33.6 Ma, as reworked Eocene microfossils have been detected in early Oligocene glacial sediment units at IODP Site U1356 and U1360 (Bijl, Houben, Bruls, et al., 2018; Houben et al., 2013). In the Australian case, U3 transforms into a conformable horizon toward the shelves and onshore regions (e.g., Frieling et al., 2018; Totterdell et al., 2000), marking the transition from thin S3 terrigenous layers to S4 carbonate platforms, without any significant hiatus formation (e.g., Totterdell et al., 2000). Similarly, a thin drape of Eocene material may have been deposited along the Antarctic shelves.

6. Summary

6.1. Mid-Jurassic to Late Cretaceous Continental Rifting (S1 and U1)

The oldest unit, S1, was deposited in sedimentary depocenters along both margins (Figure 1) during a long-term lithospheric thinning phase between Australia and Antarctica, commencing in the Middle-Late Jurassic (Bein & Taylor, 1981; Fraser & Tilbury, 1979; Willcox and Stagg, 1990). Across the Australian

margin, a series of extensional and thermal subsidence phases, with variable extension directions (both spatially and temporally), are interpreted to have controlled sediment deposition (e.g., Blevin & Cathro, 2008; Totterdell et al., 2000). The resulting successions on both margins reflect this complex history, which culminated in continental breakup at the end of sedimentary unit S1 deposition along the western and central parts of the margins. The complex structural history of this period is demonstrated by extensional faults, folding, and toe-thrust structures observed across the margins (Figures 5 and 6).

6.2. Late Cretaceous Deltaic Sedimentation (S2 and U2)

During the generally warm and humid Late Cretaceous-early Paleocene period (~94–58 Ma), large paleoriver systems on both continents transported terrigenous material into the narrow ocean basin, forming delta deposits, up to 5 km thick (Figure 7). Centers of deposition are the central GAB (Ceduna Delta) and—to a lesser extent—offshore the Antarctic Sabrina, Frost, and Astrolabe Sediment Basins (Sabrina, Frost, and Astrolabe Delta). The paleoriver systems on Australia are interpreted to have had catchment regions extending to areas more than 1,000 km away from the offshore delta. Based on our results, we suggest that the Sabrina, Frost, and Astrolabe Sediment Basins onshore Antarctica also experienced erosion in the Late Cretaceous by large river systems. It is possible that the river catchment area extended even farther inland, for example, into the Aurora, Vincennes sediment basins in the west, and/or Adventure Subglacial Trough and Wilkes sediment basin in the east (Figure 7).

6.3. Paleocene/Eocene Clockwise Ocean Currents (S3)

From ~58 Ma onward, ocean currents started to flow clockwise within the continuously widening Australian-Antarctic Basin and formed S3 contourite drifts along both margin's midslope and abyssal plain (Figure 9). The seismic character and overall morphology of these drifts indicate the same clockwise flow direction as the surface-water Proto-Leeuwin Current. Geological evidence (e.g., basin-wide glaucony and increasing evidence for current activity in drill sediments) suggest that this ocean current system strengthened and progressively penetrated farther east through the Eocene (Figure 9).

6.4. Middle-Late Eocene Decreasing Sediment Deposition (U3)

We propose that widespread decreasing sediment deposition, and partly nondeposition, occurred along both margins throughout the middle to late Eocene. Two main processes caused this strong decrease:

1. Decreasing terrigenous sediment supply offshore both margins. On the Australian margin, a combination of tectonic and climatic changes resulted in a decreasing terrigenous sediment supply (e.g., Benbow et al., 1995; Feary et al., 2000; Totterdell et al., 2000). Offshore Antarctica, increasing cooling and first formation of glaciers during the late Eocene possibly strengthened the polar high-pressure regime, producing more arid conditions (Scher et al., 2014), which may have led to decreasing fluvial runoff to the offshore basins; and
2. Strengthening of the clockwise ocean currents along the continental slopes through the Eocene, likely culminating in large-scale winnowing and depositional hiatus.

6.5. Post-Eocene Sedimentation (S4)

From about 34 Ma onward, the climate and sedimentary history of Australia and Antarctica evolves very differently. The onset of continentwide glaciation in Antarctica led to large-scale offshore sedimentary deposition (Figure 10). Thickest S4 sediments are immediately offshore and downstream of the Totten Glacier (up to 4.2 km) and to a lesser extent the Mertz and Ninnis glaciers (Figure 10), as predicted by DeConto and Pollard (2003). Structural evidence for strong down- and along-slope current activity are present particularly in the upper part of S4, for example, channel-levee systems, sediment waves, and downslope debris flows (Figures 4–6; after, e.g., De Santis et al., 2003; Close, 2010; Donda et al., 2007; Escutia et al., 1997). At the same time, Australia became semiarid, which led to very low sediment influxes and formation of thin cool-water carbonate platforms, for example, the extensive Eucla Basin (after Feary & James, 1998; Gallagher & Holdgate, 2000; Figure 10).

In summary, we find that sedimentation patterns on both Australian and Antarctic margins are broadly similar in structure and thickness, prior to the onset of Antarctic glaciation throughout the Eocene/Oligocene boundary. We infer that sedimentation on both margins was dominated by large river deltas that drained into the nascent ocean basin during the warm and humid Late Cretaceous (~94–58

Ma). On the Australian margin, deposition was concentrated offshore in the Bight and Otway basins. Deposition offshore Antarctica largely matches this pattern, with depocenters offshore the Sabrina, Frost, and Astrolabe sediment basins. The identification of drift deposits suggests ocean currents starting to circulate clockwise within the continuously widening Australian-Antarctic Basin from ~58 Ma onward. We suggest that this ocean circulation strengthened and progressed farther east through the Eocene, culminating in a drastic decrease, and partial absence of sediment deposition across the basin in the middle-late Eocene. On the Antarctic margin, this phase ended with the onset of Antarctic glaciation in the middle-late Eocene. Large amounts of glacial sediments were eroded from the coast and transported into the deeper ocean since the early Oligocene. In contrast, sediment starvation continued on the southern Australian margin, leading mainly to the formation of widespread but thin carbonate platforms on the shelves. The sediment packages we investigate here record the interactions between ancient climate, onshore drainage, and offshore ocean circulation. Our results and synthesis for the Australian-Antarctic region will provide key data sets for modeling of landscape and ocean evolution through the Cenozoic—a time of great climatic change for Australo-Antarctica.

Acknowledgments
We thank the SCAR community (Seismic Data Library System), Geoscience Australia, and Spectrum Geo Ltd for providing the seismic reflection and refraction data sets. We acknowledge IHS Markit for the provision of IHS Kingdom software used in this research. We thank Sean Gulick, German Leitchenkov, Dietmar Müller and two anonymous reviewers for the very constructive and helpful comments. Furthermore, we thank Alexey Goncharov, Howie Scher, Carlota Escutia, and Michele Rebesco for the very helpful discussions. I. S. was supported under Australian Research Council"s Special Research Initiative for Antarctic Gateway Partnership (project ID SR140300001). J. M. W. acknowledges funding from the Australian Research Council DP180102280. P.K.B. acknowledges funding through European Research Council grant no. 802835 'OceaNice'. J. M. T. publishes with the permission of the Chief Executive Officer, Geoscience Australia. The horizon grids presented in this study are available for download (DOI: 10.25959/5ba2cae0eb62a).

References

Aitken, A. R. A., Roberts, J. L., Van Ommen, T. D., Young, D. A., Golledge, N. R., Greenbaum, J. S., et al. (2016). Repeated large-scale retreat and advance of Totten Glacier indicated by inland bed erosion. *Nature*, *533*(7603), 385–389. https://doi.org/10.1038/nature17447

Aitken, A. R. A., Young, D. A., Ferraccioli, F., Betts, P. G., Greenbaum, J. S., Richter, T. G., et al. (2014). The subglacial geology of Wilkes Land, East Antarctica. *Geophysical Research Letters*, *41*, 2390–2400. https://doi.org/10.1002/2014GL059405

Amante, C. & Eakins, B. W. (2009). ETOPO1 1 arc-minute global relief model: Procedures, data sources and analysis. *NOAA Technical Memorandum NESDIS*, NGDC-24, 19 pp.

Amorosi, A. (1997). Detecting compositional, spatial, and temporal attributes of glaucony: A tool for provenance research. *Sedimentary Geology*, *109*(1-2), 135–153. https://doi.org/10.1016/S0037-0738(96)00042-5

Anderson, J. B., Warny, S., Askin, R. A., Wellner, J. S., Bohaty, S. M., Kirshner, A. E., et al. (2011). Progressive Cenozoic cooling and the demise of Antarctica's last refugium. *Proceedings of the National Academy of Sciences*, *108*(28), 11,356–11,360. https://doi.org/10.1073/pnas.1014885108

Ball, P., Eagles, G., Ebinger, C., McClay, K., & Totterdell, J. (2013). The spatial and temporal evolution of strain during the separation of Australia and Antarctica. *Geochemistry, Geophysics, Geosystems*, *14*, 2771–2799. https://doi.org/10.1002/ggge.20160

Barker, P. F. (2001). Scotia Sea regional tectonic evolution: Implications for mantle flow and palaeocirculation. *Earth-Science Reviews*, *55*(1-2), 1–39. https://doi.org/10.1016/S0012-8252(01)00055-1

Bein, J., & Taylor, M. L. (1981). The Eyre Sub-basin: Recent exploration results. *The APPEA Journal*, *21*(1), 91–98. https://doi.org/10.1071/AJ80012

Benbow, M., Alley, N., Lindsay, M., & Greenwood, D. (1995). Geological history and palaeoclimate. Geological Survey of South Australia. In J. F. Drexel, W. V. Preiss, & A. J. Parker (Eds.), *1993. The geology of South Australia: The Phanerozoic (Vol. 2). Mines and Energy, South Australia, Geological Survey of South Australia* (pp. 208–217).

Bijl, P. K., Bendle, J. A., Bohaty, S. M., Pross, J., Schouten, S., Tauxe, L., et al. (2013). Eocene cooling linked to early flow across the Tasmanian Gateway. *Proceedings of the National Academy of Sciences*, *110*(24), 9645–9650. https://doi.org/10.1073/pnas.1220872110

Bijl, P. K., Houben, A. J., Bruls, A., Pross, J., & Sangiorgi, F. (2018). Stratigraphic calibration of Oligocene-Miocene organic-walled dinoflagellate cysts from offshore Wilkes Land, East Antarctica, and a zonation proposal. *Journal of Micropalaeontology*, *37*(1), 105–138. https://doi.org/10.5194/jm-37-105-2018

Bijl, P. K., Houben, A. J., Hartman, J. D., Pross, J., Salabarnada, A., Escutia, C., & Sangiorgi, F. (2018). Paleoceanography and ice sheet variability offshore Wilkes Land, Antarctica—Part 2: Insights from Oligocene-Miocene dinoflagellate cyst assemblages. *Climate of the Past*, *14*(7), 1015–1033. https://doi.org/10.5194/cp-14-1015-2018

Bijl, P. K., Pross, J., Warnaar, J., Stickley, C. E., Huber, M., Guerstein, R., et al. (2011). Environmental forcings of Paleogene Southern Ocean dinoflagellate biogeography. *Paleoceanography*, *26*, PA1202. https://doi.org/10.1029/2009PA001905

Bijl, P. K., Sluijs, A., & Brinkhuis, H. (2013). A magneto- and chemostratigraphically calibrated dinoflagellate cyst zonation of the early Palaeogene South Pacific Ocean. *Earth-Science Reviews*, *124*, 1–31. https://doi.org/10.1016/j.earscirev.2013.04.010

Blevin, J., & Cathro, D. (2008). Australian southern margin synthesis. *Client report to Geoscience Australia by FrOG Tech Pty Ltd, Project GA707*.

Blevin, J. E. (editor) (2005). Geological framework of the Bremer and Denmark sub-basins, southwest Australia: R/V *Southern Surveyor* survey SS03/2004, Geoscience Australia Survey, 265. *Geoscience Australia Record 2005/05*.

Boeuf, M. G., & Doust, H. (1975). Structure and development of the southern margin of Australia. *The APPEA Journal*, *15*(1), 33–44. https://doi.org/10.1071/AJ74004

Bohaty, S. M., Zachos, J. C., & Delaney, M. L. (2012). Foraminiferal Mg/Ca evidence for Southern Ocean cooling across the Eocene–Oligocene transition. *Earth and Planetary Science Letters*, *317*, 251–261. https://doi.org/10.1016/j.epsl.2011.11.037

Boreham, C. J., Blevin, J. E., Duddy, I., Newman, J., Liu, K., Middleton, H. M., et al. (2002). Exploring the potential for oil generation, migration and accumulation in Cape Sorell-1, Sorell Basin, offshore West Tasmania. *The APPEA Journal*, *42*(1), 405–435. https://doi.org/10.1071/AJ01022

Bradshaw, B. E. (Compiler) (2005). Geology and petroleum prospectivity of the Bremer Sub-basin, offshore southwestern Australia. *Geoscience Australia Record*, 2005/*21*.

Brancolini, G. & Harris, P. (2000). Post-cruise report AGSO survey 217: Joint Italian/Australian marine geoscience expedition aboard the RV Tangaroa to the George Vth Land region of East Antarctica during February–March, 2000. *Australian Geological Survey Organisation*.

Cande, S. C., & Mutter, J. C. (1982). A revised identification of the oldest sea-floor spreading anomalies between Australia and Antarctica. *Earth and Planetary Science Letters*, *58*(2), 151–160. https://doi.org/10.1016/0012-821X(82)90190-X

Carter, A., Riley, T. R., Hillenbrand, C. D., & Rittner, M. (2017). Widespread Antarctic glaciation during the late Eocene. *Earth and Planetary Science Letters*, *458*, 49–57. https://doi.org/10.1016/j.epsl.2016.10.045

Close, D. I. (2010). Slope and fan deposition in deep-water turbidite systems, East Antarctica. *Marine Geology*, *274*(1-4), 21–31. https://doi.org/10.1016/j.margeo.2010.03.002

Close, D. I., Stagg, H. M. J., & O'Brien, P. E. (2007). Seismic stratigraphy and sediment distribution on the Wilkes Land and Terre Adélie margins, East Antarctica. *Marine Geology*, *239*(1-2), 34–67. https://doi.org/10.1016/j.margeo.2006.12.010

Close, D. I., Watts, A. B., & Stagg, H. M. J. (2009). A marine geophysical study of the Wilkes Land rifted continental margin, Antarctica. *Geophysical Journal International*, *177*(2), 430–450. https://doi.org/10.1111/j.1365-246X.2008.04066.x

Coffin, M. F., Frey, F. A., Wallace, P. J., & Party, S. S. (2000). Leg 183 summary: Kerguelen Plateau–Broken Ridge—A large igneous province. In *Proceedings of the Ocean Drilling Program, Initial Reports* (Vol. 183, pp. 1–101).

Colwell, J. B., Stagg, H. M., Direen, N. G., Bernardel, G., & Borissova, I. (2006). The structure of the continental margin off Wilkes Land and Terre Adelie coast, east Antarctica. In *Antarctica* (pp. 327–340). Berlin, Heidelberg: Springer. https://doi.org/10.1007/3-540-32934-X_41

Cooper, A. K., O'Brien, P. E., & ODP Leg 188 Shipboard Scientific Party (2001). Early stages of East Antarctic glaciation—Insights from drilling and seismic reflection data in the Prydz Bay region. In *The geologic record of the Antarctic ice sheet from drilling, coring and seismic studies*, Extended Abstracts (pp. 41–42). Quaderni di Geofisica.

Davies, H. L., Clarke, J. D. A., Stagg, H. M. J., Shafik, S., McGowran, B., Alley, N. F. & Willcox, J. B. (1989). Maastrichtian and younger sediments from the Great Australian Bight. *Bureau of Mineral Resources, Australia, Report 288. Australian Government Pub. Service*.

De Santis, L., Brancolini, G., & Donda, F. (2003). Seismo-stratigraphic analysis of the Wilkes Land continental margin (East Antarctica): Influence of glacially driven processes on the Cenozoic deposition. *Deep Sea Research Part II: Topical Studies in Oceanography*, *50*(8-9), 1563–1594. https://doi.org/10.1016/S0967-0645(03)00079-1

DeConto, R. M., & Pollard, D. (2003). Rapid Cenozoic glaciation of Antarctica induced by declining atmospheric CO_2. *Nature*, *421*(6920), 245–249. https://doi.org/10.1038/nature01290

Deighton, I., Falvey, D. A., & Taylor, D. J. (1976). Depositional environments and geotectonic framework: Southern Australian continental margin. *The APPEA Journal*, *16*(1), 25–36. https://doi.org/10.1071/AJ75003

Domack, E. W., Fairchild, W. W., & Anderson, J. B. (1980). Lower Cretaceous sediment from the East Antarctic continental shelf. *Nature*, *287*(5783), 625–626. https://doi.org/10.1038/287625a0

Donda, F., Brancolini, G., De Santis, L., & Trincardi, F. (2003). Seismic facies and sedimentary processes on the continental rise off Wilkes Land (East Antarctica): Evidence of bottom current activity. *Deep Sea Research Part II: Topical Studies in Oceanography*, *50*(8-9), 1509–1527. https://doi.org/10.1016/S0967-0645(03)00075-4

Donda, F., O'Brien, P. E., De Santis, L., Rebesco, M., & Brancolini, G. (2007). Mega debris flow deposits on the Western Wilkes Land margin, East Antarctica. *Antarctica: A keystone in a changing world—Online Proceedings of the 10th ISAES, USGS Open File Report, 1047*.

Ehrmann, W. U., & Mackensen, A. (1992). Sedimentological evidence for the formation of an East Antarctic ice sheet in Eocene/Oligocene time. *Palaeogeography, Palaeoclimatology, Palaeoecology*, *93*(1-2), 85–112. https://doi.org/10.1016/0031-0182(92)90185-8

Eittreim, S. L., Cooper, A. K., & Wannesson, J. (1995). Seismic stratigraphic evidence of ice-sheet advances on the Wilkes Land margin of Antarctica. *Sedimentary Geology*, *96*(1-2), 131–156. https://doi.org/10.1016/0037-0738(94)00130-M

Eittreim, S. L., & Hampton, M. A. (1987). The Antarctic continental margin: Geology and geophysics of offshore Wilkes Land. *Circum Pacific Council for Energy and Mineral Resources, Earth Science Series*, *5A*, 15–43.

Escutia, C., Brinkhuis, H., & Klaus, A. (2011). IODP Expedition 318: From greenhouse to icehouse at the Wilkes Land Antarctic margin. *Science Reports, Scientific Drilling*, *12*, 15–23. https://doi.org/10.5194/sd-12-15-2011

Escutia, C., De Santis, L., Donda, F., Dunbar, R. B., Cooper, A. K., Brancolini, G., & Eittreim, S. L. (2005). Cenozoic ice sheet history from East Antarctic Wilkes Land continental margin sediments. *Global and Planetary Change*, *45*(1-3), 51–81. https://doi.org/10.1016/j.gloplacha.2004.09.010

Escutia, C., Eittreim, S. L., Cooper, A. K., & Nelson, C. (1997). Cenozoic sedimentation on the Wilkes Land continental rise, Antarctica. In *The Antarctic region: Geological evolution and processes. Proc. Int. Symp. Antarct. Earth Sci* (Vol. 7, pp. 791–795).

Escutia, C., Nelson, C. H., Acton, G. D., Eittreim, S. L., Cooper, A. K., Warnke, D. A., & Jaramillo, J. M. (2002). Current controlled deposition on the Wilkes Land continental rise, Antarctica. *Geological Society, London, Memoirs*, *22*(1), 373–384. https://doi.org/10.1144/GSL.MEM.2002.022.01.26

Escutia, C., Warnke, D., Acton, G. D., Barcena, A., Burckle, L., Canals, M., & Frazee, C. S. (2003). Sediment distribution and sedimentary processes across the Antarctic Wilkes Land margin during the Quaternary. *Deep Sea Research Part II: Topical Studies in Oceanography*, *50*(8-9), 1481–1508. https://doi.org/10.1016/S0967-0645(03)00073-0

Espurt, N., Callot, J. P., Roure, F., Totterdell, J. M., Struckmeyer, H. I., & Vially, R. (2012). Transition from symmetry to asymmetry during continental rifting: An example from the Bight Basin–Terre Adélie (Australian and Antarctic conjugate margins). *Terra Nova*, *24*(3), 167–180. https://doi.org/10.1111/j.1365-3121.2011.01055.x

Exon, N. F., Kennett, J. P., Malone, M. J. et al. (2001). *Proceedings of the Ocean Drilling Program, Initial Reports* (Vol. 189).

Faugères, J. C., & Stow, D. A. (1993). Bottom-current-controlled sedimentation: A synthesis of the contourite problem. *Sedimentary Geology*, *82*(1-4), 287–297. https://doi.org/10.1016/0037-0738(93)90127-Q

Faugères, J. C., & Stow, D. A. V. (2008). Contourite drifts: Nature, evolution and controls. *Developments in Sedimentology*, *60*, 257–288. https://doi.org/10.1016/S0070-4571(08)10014-0

Feary, D. A., Hine, A. C., Malone, M. J., Andres, M., Betzler, C., Brooks, G. R., et al. (2000). Great Australian Bight: Cenozoic cool-water carbonates. In *Proceedings of the Ocean Drilling Program, Initial Reports* (Vol. *182*, pp. 1–5).

Feary, D. A., & James, N. P. (1998). Seismic stratigraphy and geological evolution of the Cenozoic, cool-water Eucla Platform, Great Australian Bight. *AAPG Bulletin*, *82*(5), 792–816. https://doi.org/10.1306/1d9bc601-172d-11d7-8645000102c1865d

Fraser, A. R., & Tilbury, L. A. (1979). Structure and stratigraphy of the Ceduna Terrace region, Great Australian Bight basin. *The APPEA Journal*, *19*(1), 53–65. https://doi.org/10.1071/AJ78007

Fretwell, P., Pritchard, H. D., Vaughan, D. G., Bamber, J. L., Barrand, N. E., Bell, R., et al. (2012). Bedmap2: Improved ice bed, surface and thickness datasets for Antarctica. *The Cryosphere Discussions*, *6*(5), 4305–4361. https://doi.org/10.5194/tcd-6-4305-2012

Frieling, J., Huurdeman, E., Rem, C., Donders, T. H., Pross, J., Bohaty, S. M., et al. (2018). Identification of the Paleocene-Eocene boundary in coastal strata in the Otway Basin, Victoria, Australia. *Journal of Micropalaeontology*, *37*(1), 317–339. https://doi.org/10.5194/jm-37-317-2018

Gallagher, S. J., & Holdgate, G. (2000). The palaeogeographic and palaeoenvironmental evolution of a Palaeogene mixed carbonate–siliciclastic cool-water succession in the Otway Basin, Southeast Australia. *Palaeogeography, Palaeoclimatology, Palaeoecology*, *156*(1-2), 19–50. https://doi.org/10.1016/S0031-0182(99)00130-3

Gillard, M., Autin, J., Manatschal, G., Sauter, D., Munschy, M., & Schaming, M. (2015). Tectonomagmatic evolution of the final stages of rifting along the deep conjugate Australian-Antarctic magma-poor rifted margins: Constraints from seismic observations. *Tectonics*, *34*, 753–783. https://doi.org/10.1002/2015TC003850

Gingele, F. X., & De Deckker, P. (2005). Clay mineral, geochemical and Sr–Nd isotopic fingerprinting of sediments in the Murray–Darling fluvial system, southeast Australia. *Australian Journal of Earth Sciences*, *52*(6), 965–974. https://doi.org/10.1080/08120090500302301

Gradstein, F. M., Ogg, J. G., Schmitz, M., & Ogg, G. (2012). *The geologic time scale 2012* (p. 1144). Elsevier.

Gulick, S. P., Shevenell, A. E., Montelli, A., Fernandez, R., Smith, C., Warny, S., et al. (2017). Initiation and long-term instability of the East Antarctic Ice Sheet. *Nature*, *552*(7684), 225–229. https://doi.org/10.1038/nature25026

Hall, J. W., Glorie, S., Collins, A. S., Reid, A., Evans, N., McInnes, B., & Foden, J. (2016). Exhumation history of the Peake and Denison Inliers: Insights from low-temperature thermochronology. *Australian Journal of Earth Sciences*, *63*(7), 805–820. https://doi.org/10.1080/08120099.2016.1253615

Hay, W. W., & DeConto, R. M. (1999). Comparison of modern and Late Cretaceous meridional energy transport and oceanology. In E. Barrera & C. C. Johnson (Eds.), *Evolution of the Cretaceous ocean-climate system*, *Geological Society of America, Special Papers* (Vol. 332, pp. 283–300).

Hayes, D. E. (1975) and the Expedition 28 Scientists. General synthesis, deep sea drilling project leg 28. *Initial Reports of the Deep Sea Drilling Project*, *28*, 919-942.

Hill, P. J., Moore, A. M. G., & Exon, N. F. (2001). Sedimentary basins and structural framework of the South Tasman Rise and East Tasman Plateau. *Geoscience Australia*, *Record 2001/40*.

Houben, A. J., Bijl, P. K., Guerstein, G. R., Sluijs, A., & Brinkhuis, H. (2011). *Malvinia escutiana*, a new biostratigraphically important Oligocene dinoflagellate cyst from the Southern Ocean. *Review of Palaeobotany and Palynology*, *165*(3-4), 175–182. https://doi.org/10.1016/j.revpalbo.2011.03.002

Houben, A. J., Bijl, P. K., Pross, J., Bohaty, S. M., Passchier, S., Stickley, C. E., et al. (2013). Reorganization of Southern Ocean plankton ecosystem at the onset of Antarctic glaciation. *Science*, *340*(6130), 341–344. https://doi.org/10.1126/science.1223646

Houben, A. J., Bijl, P. K., Sluijs, A., Schouten, S., & Brinkhuis, H. (2019). Late Eocene Southern Ocean cooling and invigoration of circulation preconditioned Antarctica for full-scale glaciation. *Geochemistry, Geophysics, Geosystems*, *20*, 2214–2234. https://doi.org/10.1029/2019GC008182

Huber, B. T., Hobbs, R. W., Bogus, K. A., & the Expedition 369 Scientists (2018). *Expedition 369 preliminary report: Australia Cretaceous climate and tectonics*. *International Ocean Discovery Program*.

Huber, B. T., Hodell, D. A., & Hamilton, C. P. (1995). Middle–Late Cretaceous climate of the southern high latitudes: Stable isotopic evidence for minimal equator-to-pole thermal gradients. *Geological Society of America Bulletin*, *107*(10), 1164–1191. https://doi.org/10.1130/0016-7606(1995)107<1164:MLCCOT>2.3.CO;2

Huber, M., Brinkhuis, H., Stickley, C. E., Döös, K., Sluijs, A., Warnaar, J., et al. (2004). Eocene circulation of the Southern Ocean: Was Antarctica kept warm by subtropical waters? *Paleoceanography*, *19*, PA4026. https://doi.org/10.1029/2004PA001014

Hüneke, H., & Stow, D. A. V. (2008). Identification of ancient contourites: Problems and palaeoceanographic significance. *Developments in Sedimentology*, *60*, 323–344.

Jamieson, S. S., Sugden, D. E., & Hulton, N. R. (2010). The evolution of the subglacial landscape of Antarctica. *Earth and Planetary Science Letters*, *293*(1-2), 1–27. https://doi.org/10.1016/j.epsl.2010.02.012

Jamieson, S. S. R., Hulton, N. R. J., Sugden, D. E., Payne, A. J., & Taylor, J. (2005). Cenozoic landscape evolution of the Lambert basin, East Antarctica: The relative role of rivers and ice sheets. *Global and Planetary Change*, *45*(1-3), 35–49. https://doi.org/10.1016/j.gloplacha.2004.09.015

Jamieson, S. S. R., & Sugden, D. E. (2008). Landscape evolution of Antarctica. In A. K. Cooper, P. Barrett, H. Stagg, B. Storey, E. Sump, W. Wise, & 10th ISAES Editorial Team (Eds.), *Antarctica: A keystone in a changing world* (pp. 39–54). USA: The National Academic Press.

Kennett, J. P., Houtz, R. E., Andrews, P. B., Edwards, A. R., Gostin, V. A., Hajós, M., et al. (1974). *Initial reports of the Deep Sea Drilling Project* (Vol. *29*). Washington: U.S. Government Printing Office.

King, S. J., & Mee, B. C. (2004). The seismic stratigraphy and petroleum potential of the Late Cretaceous Ceduna Delta, Ceduna Sub-basin, Great Australian Bight. In P. J. Boult, D. R. Johns, & S. C. Lang (Eds.), *Eastern Australasian basins symposium II* (pp. 63–73). Petroleum Exploration Society of Australia, Special Publication.

Krassay, A. A., Cathro, D. L., & Ryan, D. J. (2004). A regional tectonostratigraphic framework for the Otway Basin. In P. J. Boult, D. R. Johns, & S. C. Lang (Eds.), *Eastern Australasian basins symposium II* (pp. 97–116). Petroleum Exploration Society of Australia, Special Publication.

Krassay, A. A., & Totterdell, J. M. (2003). Seismic stratigraphy of a large, Cretaceous shelf-margin delta complex, offshore southern Australia. *AAPG Bulletin*, *87*(6), 935–963. https://doi.org/10.1306/01240300015

Lane, H., Müller, R. D., Totterdell, J. M., & Whittaker, J. M. (2012). Developing a consistent sequence stratigraphy for the Wilkes Land and Great Australian Bight margins. *Eastern Australasian basins symposium IV*. Petroleum Exploration Society of Australia.

Leitchenkov, G. L., & Guseva, Y. B. (2012). In Russian. Seismic stratigraphy of the Southern Indian Ocean and reconstruction of paleoenvironments/Сейсмостратиграфия осадочного чехла индоокеанской акватории Антарктики и реконструкция природной среды в геологическом прошлом. *Разведка и охрана недр*, *8*, 21–29.

Leitchenkov, G. L., Guseva, Y. B., & Gandyukhin, V. V. (2007). Cenozoic environmental changes along the East Antarctic continental margin inferred from regional seismic stratigraphy. In *Antarctica: A keystone in a changing world. Proc. 10th Int. Symp. on Antarctic Earth Science. USGS–US National Academy*.

Leitchenkov, G. L., Guseva, Y. B., Gandyukhin, V. V., & Ivanov, S. V. (2015). In Russian. *Crustal structure, tectonic evolution and seismic stratigraphy of the Southern Indian Ocean/СТРОЕНИЕ ЗЕМНОЙ КОРЫ И ИСТОРИЯ ГЕОЛОГИЧЕСКОГО РАЗВИТИЯ ОСАДОЧНЫХ БАССЕЙНОВ ИНДООКЕАНСКОЙ АКВАТОРИИ АНТАРКТИКИ*. St. Petersburg: Academy Publishing Center. ISBN: 978-5-88994-117-0.

Linnert, C., Robinson, S. A., Lees, J. A., Bown, P. R., Prez-Rodrguez, I., Petrizzo, M. R., et al. (2014). Evidence for global cooling in the Late Cretaceous. *Nature Communications*, *5*, 4194.

Livermore, R., Nankivell, A., Eagles, G., & Morris, P. (2005). Paleogene opening of Drake passage. *Earth and Planetary Science Letters*, *236*(1-2), 459–470. https://doi.org/10.1016/j.epsl.2005.03.027

Lloyd, J., Collins, A. S., Payne, J. L., Glorie, S., Holford, S., & Reid, A. J. (2016). Tracking the Cretaceous transcontinental Ceduna River through Australia: The hafnium isotope record of detrital zircons from offshore southern Australia. *Geoscience Frontiers*, *7*(2), 237–244. https://doi.org/10.1016/j.gsf.2015.06.001

MacDonald, J., King, R., Hillis, R., & Backé, G. (2010). Structural style of the White Pointer and Hammerhead Delta—Deepwater fold-thrust belts, Bight Basin, Australia. *The APPEA Journal*, *50*(1), 487–510. https://doi.org/10.1071/AJ09029

Mantle, D. J., Totterdell, J. M., Struckmeyer, H. I. M., & Kelman, A. P. (2009). Chart 35: Bight Basin Biozonation and Stratigraphy. Geoscience Australia.

McGowran, B., Li, Q., Cann, J., Padley, D., McKirdy, D. M., & Shafik, S. (1997). Biogeographic impact of the Leeuwin Current in southern Australia since the late middle Eocene. *Palaeogeography, Palaeoclimatology, Palaeoecology*, *136*(1-4), 19–40. https://doi.org/10.1016/S0031-0182(97)00073-4

McRae, S. G. (1972). Glauconite. *Earth-Science Reviews*, *8*(4), 397–440. https://doi.org/10.1016/0012-8252(72)90063-3

Messent, B. E. (1998). Great Australian Bight: Well Auit. *Australian Geological Survey Organisation, Record 1998/37*.

Miller, G., Kominz, M. A., Browning, J. V., Wright, J. D., Mountain, G. S., Katz, M. E., et al. (2005). The Phanerozoic record of global sea-level change. *Science*, *310*(5752), 1293–1298. https://doi.org/10.1126/science.1116412

Monteil, E., Macphail, M., Howe, R., Boreham, C., O'Leary, R., Davenport, R. & Hong, Z. (2005). Post-survey analytical results: Biostratigraphic results—Palynology. In J. E. Blevin (Ed.), *Geological framework of the Bremer and Denmark sub-basins, southwest Australia*: R/V *Southern Surveyor* Survey SS03/04, Geoscience Australia Survey 265, post-survey report. *Geoscience Australia, Record 2005/05*, 47–50.

Morgan, R., Alley, N. F., Rowett, A. I., & White, M. R. (1995). Biostratigraphy, Chapter 6. In J. G. G. Morton & J. F. Drexel (Eds.), *The petroleum geology of South Australia*. Volume 1: Otway Basin, South Australian Department of Mines and Energy, *Report Book 95/15*, pp.95-101.

Mutti, E. & Carminatti, M. (2011). Deep-water sands of the Brazilian offshore basins. *In AAPG International Conference and Exhibition, Milan, Italy* (pp. 1-42).

Odin, G. S. & Fullagar, P. D. (1988). Chapter C4 Geological significance of the glaucony facies. In *Developments in Sedimentology* (Vol. *45*, pp. 295-332). Elsevier. https://doi.org/10.1016/S0070-4571(08)70069-4

Odin, G. S., & Matter, A. (1981). De glauconiarum origine. *Sedimentology*, *28*(5), 611–641. https://doi.org/10.1111/j.1365-3091.1981.tb01925.x

Passchier, S., Bohaty, S. M., Jiménez-Espejo, F., Pross, J., Röhl, U., Van De Flierdt, T., et al. (2013). Early Eocene to middle Miocene cooling and aridification of East Antarctica. *Geochemistry, Geophysics, Geosystems*, *14*, 1399–1410. https://doi.org/10.1002/ggge.20106

Pollack, R. M. (2003). PhD thesis. Sequence stratigraphy of the Paleocene to Miocene Gambier Sub-Basin, Southern Australia. University of Adelaide, Adelaide, Australia.

Raza, A., Hill, K. C., & Korsch, R. J. (2009). Mid-Cretaceous uplift and denudation of the Bowen and Surat Basins, eastern Australia: Relationship to Tasman Sea rifting from apatite fission-track and vitrinite-reflectance data. *Australian Journal of Earth Sciences*, *56*(3), 501–531. https://doi.org/10.1080/08120090802698752

Rebesco, M., & Camerlenghi, A. e. (2008). *Contourites* (Vol. 60). Elsevier.

Rebesco, M., Hernández-Molina, F. J., Van Rooij, D., & Wåhlin, A. (2014). Contourites and associated sediments controlled by deep-water circulation processes: State-of-the-art and future considerations. *Marine Geology*, *352*, 111–154. https://doi.org/10.1016/j.margeo.2014.03.011

Robson, A. G., King, R. C., & Holford, S. P. (2016). 3D seismic analysis of gravity-driven and basement influenced normal fault growth in the deepwater Otway Basin, Australia. *Journal of Structural Geology*, *89*, 74–87. https://doi.org/10.1016/j.jsg.2016.06.002

Sangiorgi, F., Bijl, P. K., Passchier, S., Salzmann, U., Schouten, S., McKay, R., et al. (2018). Southern Ocean warming and Wilkes Land ice sheet retreat during the mid-Miocene. *Nature Communications*, *9*(1), 317. https://doi.org/10.1038/s41467-017-02609-7

Scher, H. D., Bohaty, S. M., Smith, B. W., & Munn, G. H. (2014). Isotopic interrogation of a suspected late Eocene glaciation. *Paleoceanography and Paleoclimatology*, *29*, 628–644. https://doi.org/10.1002/2014PA002648

Scher, H. D., Whittaker, J. M., Williams, S. E., Latimer, J. C., Kordesch, W. E., & Delaney, M. L. (2015). Onset of Antarctic circumpolar current 30 million years ago as Tasmanian Gateway aligned with westerlies. *Nature*, *523*(7562), 580–583. https://doi.org/10.1038/nature14598

Shafik, S. (1973). Eocene-Oligocene nannoplankton biostratigraphy in the western and southern margins of Australia. Abstract. In *45th Congress. Australia & New Zealand Association for the Advancement of Science. Section* (Vol. *3*, pp. 101-103).

Shafik, S. (1983). Calcareous nannofossil biostratigraphy: an assessment of foraminiferal events in the Eocene of the Otway Basin, Southeastern Australia. *BMR Journal of Australian Geology and Geophysics*, *8*, 1–18.

Shafik, S. (1990). The Maastrichtian and early Tertiary record of the Great Australian Bight Basin and its onshore equivalents on the Australian southern margin: A nannofossil study. *BMR Journal of Australian Geology and Geophysics*, *11*, 473–497.

Shafik, S. (1992). Eocene and Oligocene calcareous nannofossils from the Great Australian Bight: Evidence of significant reworking episodes and surface-water temperature changes. *BMR Journal of Australian Geology and Geophysics*, *13*, 131–142.

Shanmugam, G. (2000). 50 years of the turbidite paradigm (1950s–1990s): Deep-water processes and facies models—a critical perspective. *Marine and petroleum Geology*, *17*(2), 285–342.

Shanmugam, G. (2017). Contourites: Physical oceanography, process sedimentology, and petroleum geology. *Petroleum Exploration and Development*, *44*(2), 183–216.

Sijp, W. P., Anna, S., Dijkstra, H. A., Flögel, S., Douglas, P. M., & Bijl, P. K. (2014). The role of ocean gateways on cooling climate on long time scales. *Global and Planetary Change*, *119*, 1–22. https://doi.org/10.1016/j.gloplacha.2014.04.004

Sijp, W. P., England, M. H., & Huber, M. (2011). Effect of the deepening of the Tasman Gateway on the global ocean. *Paleoceanography*, *26*, PA4207. https://doi.org/10.1029/2011PA002143

Sijp, W. P., von der Heydt, A. S., & Bijl, P. K. (2016). Model simulations of early westward flow across the Tasman Gateway during the early Eocene. *Climate of the Past*, *12*(4), 807–817. https://doi.org/10.5194/cp-12-807-2016

Sluijs, A., Brinkhuis, H., Stickley, C. E., Warnaar, J., Williams, G. L. & Fuller, M. (2003). Dinoflagellate cysts from the Eocene/Oligocene transition in the Southern Ocean; Results from ODP Leg 189. In *Proceedings of the Ocean Drilling Program. Scientific Results*.

Stacey, A., Mitchell, C., Nayak, G., Struckmeyer, H., Morse, M., Totterdell, J., & Gibson, G. (2013). Geology and petroleum prospectivity of the deepwater Otway and Sorell basins: New insights from an integrated regional study. *The APPEA Journal*, *51*(2), 692–692.

Stagg, H. M. J., Cockshell, C. D., Willcox, J. B., Hill, A. J., Needham, D. J. L., Thomas, B., et al. (1990). Basins of the Great Australian Bight region: Geology and petroleum potential. *Bureau of Mineral Resources, Geology and Geophysics, Australia, Continental Margins Program, Folio 5: text. Australian Government Publishing Service*.

Stagg, H. M. J., Colwell, J. B., Direen, N. G., O'Brien, P. E., Browning, B. J., Bernardel, G., et al. (2005). Geological framework of the continental margin in the region of the Australian Antarctic Territory. *Geoscience Australia Record*, *2004*, 1–373.

Stanley, D. J. (1993). Model for turbidite-to-contourite continuum and multiple process transport in deep marine settings: Examples in the rock record. *Sedimentary Geology*, *82*(1-4), 241–255. https://doi.org/10.1016/0037-0738(93)90124-N

Stickley, C. E., Brinkhuis, H., Schellenberg, S. A., Sluijs, A., Röhl, U., Fuller, M., et al. (2004). Timing and nature of the deepening of the Tasmanian Gateway. *Paleoceanography*, *19*, PA4027. https://doi.org/10.1029/2004PA001022

Stocchi, P., Escutia, C., Houben, A. J., Vermeersen, B. L., Bijl, P. K., Brinkhuis, H., et al. (2013). Relative sea-level rise around East Antarctica during Oligocene glaciation. *Nature Geoscience*, *6*(5), 380–384. https://doi.org/10.1038/ngeo1783

Stow, D. A., Faugères, J. C., Howe, J. A., Pudsey, C. J., & Viana, A. R. (2002). Bottom currents, contourites and deep-sea sediment drifts: Current state-of-the-art. *Geological Society, London, Memoirs*, *22*(1), 7–20. https://doi.org/10.1144/GSL.MEM.2002.022.01.02

Stow, D. A., Kahler, G., & Reeder, M. (2002). Fossil contourites: Type example from an Oligocene palaeoslope system, Cyprus. *Geological Society, London, Memoirs*, *22*(1), 443–455. https://doi.org/10.1144/GSL.MEM.2002.022.01.31

Stow, D. A. V., & Faugères, J. C. (2008). Contourite facies and the facies model. *Developments in Sedimentology*, *60*, 223–256. https://doi.org/10.1016/S0070-4571(08)10013-9

Stow, D. A. V., & Lovell, J. P. B. (1979). Contourites: Their recognition in modern and ancient sediments. *Earth-Science Reviews*, *14*(3), 251–291. https://doi.org/10.1016/0012-8252(79)90002-3

Strand, K., Passchier, S., & Näsi, J. (2003). Implications of quartz grain microtextures for onset Eocene/Oligocene glaciation in Prydz Bay, ODP Site 1166, Antarctica. *Palaeogeography, Palaeoclimatology, Palaeoecology*, *198*(1-2), 101–111. https://doi.org/10.1016/S0031-0182(03)00396-1

Tanahashi, M., Ishihara, T., Yuasa, M., Murakami, F., & Nishimura, A. (1997). Preliminary report of the TH95 geological and geophysical survey results in the Ross Sea and Dumont D'Urville Sea. *NIPR Symposium on Antarctic Geosciences, Proceedings*, *10*, 57–58.

Tauxe, L., Stickley, C. E., Sugisaki, S., Bijl, P. K., Bohaty, S. M., Brinkhuis, H., et al. (2012). Chronostratigraphic framework for the IODP Expedition 318 cores from the Wilkes Land Margin: Constraints for paleoceanographic reconstruction. *Paleoceanography and Paleoclimatology*, 27, PA2214. https://doi.org/10.1029/2012pa002308

Tikku, A. A., & Cande, S. C. (1999). The oldest magnetic anomalies in the Australian-Antarctic Basin: Are they isochrons? *Journal of Geophysical Research - Solid Earth*, *104*(B1), 661–677. https://doi.org/10.1029/1998JB900034

Totterdell, J. M., Blevin, J. E., Struckmeyer, H. I. M., Bradshaw, B. E., Colwell, J. B., & Kennard, J. M. (2000). A new sequence framework for the Great Australian Bight: Starting with a clean slate. *The APPEA Journal*, *40*(1), 95–118. https://doi.org/10.1071/AJ99007

Totterdell, J. M., & Bradshaw, B. E. (2004). The structural framework and tectonic evolution of the Bight Basin. In *Eastern Australasian basins symposium II* (pp. 41–61). Petroleum Exploration Society of Australia, Special Publication.

Totterdell, J. M., Hall, L., Hashimoto, T., Owen, K. & Bradshaw, M. T. (2014). Petroleum geology inventory of Australia's offshore frontier basins. *Record 2014/09, Geoscience Australia, Canberra. Journal, 42*, 405-435.

Totterdell, J. M. & Krassay, A. A. (2003a). Sequence stratigraphic correlation of onshore and offshore Bight Basin successions. *Geoscience Australia Record,* 2.

Totterdell, J. M., & Krassay, A. A. (2003b). The role of shale deformation and growth faulting in the Late Cretaceous evolution of the Bight Basin, offshore southern Australia. *Geological Society, London, Special Publications*, *216*(1), 429–442. https://doi.org/10.1144/GSL.SP.2003.216.01.28

Truswell, E. M. (1982). Palynology of seafloor samples collected by the 1911–14 Australasian Antarctic Expedition: Implications for the geology of coastal East Antarctica. *Journal of the Geological Society of Australia*, *29*(3-4), 343–356. https://doi.org/10.1080/00167618208729218

Tsumuraya, Y., Tanahashi, M., Saki, T., Machihara, T., & Asakura, N. (1985). Preliminary report of the marine geophysical and geological surveys off Wilkes Land, Antarctica in 1983–1984. *Memoirs of National Institute of Polar Research*, Special Issue, *37*, 48–62.

Veevers, J. (2001). *Atlas of billion-year earth history of Australia and neighbours in Gondwanaland*, (p. 388). Sydney: Department of Earth and Planetary Sciences Press.

Viana, A. R., Faugères, J. C., & Stow, D. A. V. (1998). Bottom-current-controlled sand deposits—a review of modern shallow-to deep-water environments. *Sedimentary Geology*, *115*(1-4), 53–80. https://doi.org/10.1016/S0037-0738(97)00087-0

Wannesson, J., Pelras, M., Petitperrin, B., Perret, M., & Segoufin, J. (1985). A geophysical transect of the Adelie Margin, East Antarctica. *Marine and Petroleum Geology*, *2*(3), 192–200. https://doi.org/10.1016/0264-8172(85)90009-1

Wardell, N., Childs, J. R. & Cooper, A. K. (2007). Advances through collaboration: Sharing seismic reflection data via the Antarctic Seismic Data Library System for Cooperative Research (SDLS). *Antarctica: A keystone in a changing world—Online proceedings of the 10th ISAES: USGS Open-File Report, 1047*.

Wei, W. (2004). Opening of the Australia–Antarctica Gateway as dated by nannofossils. *Marine Micropaleontology*, *52*(1-4), 133–152. https://doi.org/10.1016/j.marmicro.2004.04.008

Whittaker, J. M., Goncharov, A., Williams, S. E., Müller, R. D., & Leitchenkov, G. (2013). Global sediment thickness data set updated for the Australian-Antarctic Southern Ocean. *Geochemistry, Geophysics, Geosystems*, *14*, 3297–3305. https://doi.org/10.1002/ggge.20181

Whittaker, J. M., Müller, R. D., Leitchenkov, G., Stagg, H., Sdrolias, M., Gaina, C., & Goncharov, A. (2007). Major Australian-Antarctic plate reorganization at Hawaiian-Emperor bend time. *Science*, *318*(5847), 83–86. https://doi.org/10.1126/science.1143769

Whittaker, J. M., Williams, S. E., & Müller, R. D. (2013). Revised tectonic evolution of the Eastern Indian Ocean. *Geochemistry, Geophysics, Geosystems*, *14*, 1891–1909. https://doi.org/10.1002/ggge.20120

Willcox, J. B., & Stagg, H. M. J. (1990). Australia's southern margin: A product of oblique extension. *Tectonophysics*, *173*(1-4), 269–281. https://doi.org/10.1016/0040-1951(90)90223-U

Zachos, J. C., Dickens, G. R., & Zeebe, R. E. (2008). An early Cenozoic perspective on greenhouse warming and carbon-cycle dynamics. *Nature*, *451*(7176), 279–283. https://doi.org/10.1038/nature06588

Zachos, J. C., Stott, L. D., & Lohmann, K. C. (1994). Evolution of early Cenozoic marine temperatures. *Paleoceanography*, *9*(2), 353–387. https://doi.org/10.1029/93PA03266